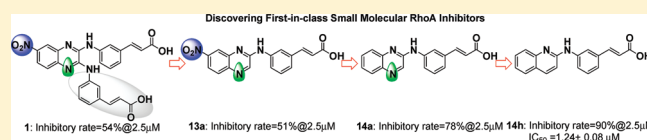


Design and Synthesis of Small Molecule RhoA Inhibitors:
A New Promising Therapy for Cardiovascular Diseases?Jing Deng,^{†,||} Enguang Feng,^{†,||} Sheng Ma,^{§,||} Yan Zhang,[§] Xiaofeng Liu,[†] Honglin Li,^{*,†} Huang Huang,[†] Jin Zhu,[†] Weiliang Zhu,[‡] Xu Shen,^{†,‡} Liyan Miao,^{*,§} Hong Liu,[‡] Hualiang Jiang,^{†,‡} and Jian Li^{*,†}[†]School of Pharmacy, East China University of Science and Technology, 130 Mei Long Road, Shanghai 200237, China[‡]Drug Discovery and Design Center, Shanghai Institute of Materia Medica, Chinese Academy of Sciences, 555 Zu Chong Zhi Road, Shanghai 201203, China[§]Department of Clinical Pharmacology Research Lab, The First Affiliated Hospital of Soochow University, 188 Shi Zhi Street, Suzhou 215006, China

S Supporting Information

ABSTRACT: RhoA is a member of Rho GTPases, a subgroup of the Ras superfamily of small GTP-binding proteins. RhoA, as an important regulator of diverse cellular signaling pathways, plays significant roles in cytoskeletal organization, transcription, and cell-cycle progression. The RhoA/ROCK inhibitors have emerged as a new promising treatment for cardiovascular diseases. However, to date, RhoA inhibitors are macromolecules, and to our knowledge, small molecular-based inhibitors have not been reported. In this study, a series of first-in-class small molecular RhoA inhibitors have been discovered by using structure-based virtual screening in conjunction with chemical synthesis and bioassay. Virtual screening of ~200,000 compounds, followed by SPR-based binding affinity assays resulted in three compounds with binding affinities to RhoA at the micromolar level (compounds 1–3). Compound 1 was selected for further structure modifications in considering binding activity and synthesis ease. Forty-one new compounds (1, 12a–v, 13a–h, and 14a–j) were designed and synthesized accordingly. It was found that eight (12a, 12j, 14a, 14b, 14d, 14e, 14g, and 14h) showed high RhoA inhibition activities with IC₅₀ values of 1.24 to 3.00 μM. A pharmacological assay indicated that two compounds (14g and 14h) demonstrated noticeable vasorelaxation effects against PE-induced contraction in thoracic aorta artery rings and served as good leads for developing more potent cardiovascular agents.



1. INTRODUCTION

Rho family proteins are members of the main branches of the Ras superfamily of small GTPases.¹ Rho GTPases, including Rho, Rac, and Cdc42, regulate the actin cytoskeleton² and several signaling pathways.³ RhoA, as one of the most well characterized members, is essential for multiple cellular processes including cytoskeletal rearrangement, gene expression, and membrane trafficking, as well as cell adhesion, migration, differentiation, proliferation, and apoptosis.^{4–6}

RhoA, similar to all GTPases, functions as bimolecular switch that cycles between active GTP-bound and inactive GDP-bound forms. When activated, RhoA is able to interact with diverse effectors to carry out its cellular functions. To date, the best-characterized downstream target of RhoA is Rho kinase (ROCK). Within cardiovascular system, regulation of vascular tone is mainly dependent on two pathways (Figure 1): the Ca²⁺-dependent vasoconstriction by activation of the myosin light chain kinase (MLCK), and the Rho-ROCK-mediated Ca²⁺ sensitization, which can occur independently of intracellular Ca²⁺ changes.^{7,8} In 1990s, RhoA was identified as the upstream mediator of Ca²⁺ sensitization, and RhoA/ROCK activation leads to inhibition of myosin light chain phosphatase (MLCP). The event can also produce directly phosphorylation of MLC, resulting in an synergistic

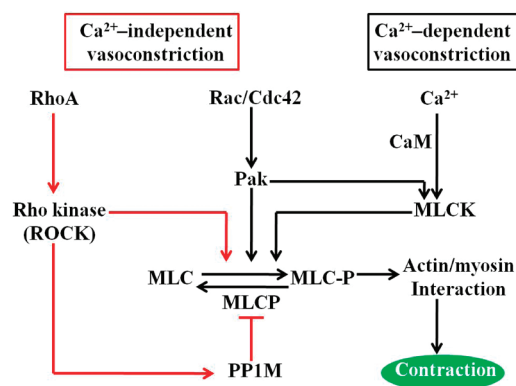


Figure 1. Two regulatory pathways (Ca²⁺-dependent and Ca²⁺-independent) of vasoconstriction.

increase of vascular tone (red arrows in Figure 1).⁹ Therefore, the connection between RhoA/ROCK activation and vasoconstriction has made the inhibition of the RhoA pathway an appealing target for pharmacological treatment of numerous cardiovascular

Received: January 28, 2011

Published: May 26, 2011

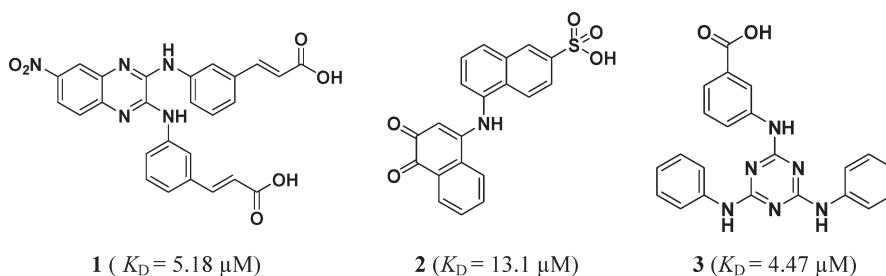


Figure 2. Structures of 3 binders (or hits) of RhoA selected from the candidates by virtual screening and the SPR-based binding affinity assay.

disorders, including hypertension, coronary and cerebral vasospasm, atherosclerosis, vascular aneurisms, diabetes, stroke, and heart failure.^{10–12} In addition, it is also a valuable target for the treatment of cancer,^{13–16} nervous system disease,¹⁷ and asthma.¹⁸

Among ROCK inhibitors, Fasudil is an approved drug for cerebral vasospasm after subarachnoid hemorrhage and a number of other ROCK inhibitors, such as Y-27632 and statins, have also been reported in the literature.^{19–24} Despite the significant progress, very limited efforts have been devoted toward the development of direct RhoA inhibitors, especially small molecular inhibitors have not been reported.

Clostridium botulinum C3 exoenzyme and the related transferases have been used as a tool to inactivate RhoA and to analyze cellular functions of Rho proteins.²⁵ Nevertheless, C3 transferase with about 25–30 kDa, only consists of one enzyme domain and lacks a cell binding and transport domain.^{26,27} Its extremely low efficiency of cell entry and degradation in vivo has restricted the therapeutic value. Instead, much effort has been paid for C3 transferase. Tan et al. developed a membrane-permeating form of C3 transferase (TAT-C3) and a biopolymer-based microsphere depot system for sustainable controlled release of the protein to suit the pattern of RhoA expression in injured central nervous.²⁸ Lord-Fontaine et al. reported an improved cell-permeable C3 variant (BA-210), expected to provide significant neuroprotective and neuroregenerative benefits.²⁹ In addition, Town et al. described a novel RhoA inhibitor (a Gli3-regulated, transmembrane protein) that directed cell migration and actin polymerization and was implicated in lip and palate formation.³⁰ These results highlight the potential of RhoA as a therapeutic target in the treatment of cardiovascular diseases.

Small molecules are highly valuable for developing clinically useful agents. Toward this end, recently we initiated a program aimed at seeking the first-in-class small molecule RhoA inhibitors. By using a docking-based virtual screening approach in conjunction with surface plasmon resonance (SPR) determination, three novel small molecule RhoA binders (hits) (compounds **1–3**, Figure 2) have been discovered. According to the binding potency and synthetic complexity, compound **1** was selected as the starting point for further structural optimization. Totally, 41 new compounds have been designed, synthesized, and tested with biological assays. Finally, eight compounds (**12a**, **12j**, **14a–b**, **14d–e**, and **14g–4h**) were found to show high RhoA inhibition activities, and two compounds (**14g** and **14h**) showed significant inhibitory effects against phenylephrine (PE)-induced contraction in thoracic aorta artery rings. To our knowledge, the two compounds are the first-in-class small molecular RhoA inhibitors.

2. MATERIALS AND METHODS

2.1. Computation. **2.1.1. Virtual Screening.** The virtual screening was performed on the vendor database from SPECS

(Specs: Chemistry Solutions for Drug Discovery, 2008; <http://www.specs.net/> (accessed October 1, 2007)), which involves ~200,000 compounds. All the compounds containing inorganic atoms were removed prior to the screening. The remaining molecules are prepared (including adding hydrogen atoms, ionizing at the pH range from 6.0 to 9.0, generating stereo isomers and valid single 3D conformers) by means of the Ligand Preparation module in Discovery Studio 2.0 (Accelrys, Inc.).

A hierarchical virtual screening strategy was adopted. The crystal structure of RhoA was retrieved from the Protein Data Bank (PDB entry: 1KMQ). Amino acid residues located within 8.0 Å from the complexed ligand GNP were defined as part of the binding site for docking studies. All crystallographic water molecules were removed from the coordinate set. DOCK4.0^{31,32} was used for the initial screening. Hydrogen atoms and Amber charges of the receptor were added with Chimera (<http://www.cgl.ucsf.edu/chimera>). The grid-enclosing box was generated around the binding site defined previously. In the docking process, the standard DOCK score was used to rank the result list. All the parameters were set as the default values. The top ranked 3000 candidates were reserved for detail docking and reranking with Glide (Schrödinger, Inc.) in standard precision (SP) mode. The grid-enclosing box was centered on the centroid of cocomplexed GNP in RhoA and defined so as to enclose residues located within 14.0 Å around the GNP binding site, and a scaling factor of 1.0 was set to van der Waals (VDW) radii of those receptor atoms with the partial atomic charge less than 0.25. After visual observation of corresponding binding modes, 54 compounds were selected and purchased from the vendor for the bioassay.

2.1.2. Molecular Docking. The binding poses of compound **1** and the most potent synthesized compound **14h** were modeled by Glide in SP mode with the same parameter settings in virtual screening.

2.2. Chemistry. **2.2.1. Design of Analogues of Compound 1.** Compounds **1–3** (Figure 2) showing high binding affinities to RhoA were obtained by SPR determination (see section 3) from the 120 candidate compounds selected by virtual screening. Compound **1** with the potent binding affinity and easy synthetic accessibility was used as lead compound for designing new RhoA inhibitors. To provide expedient and significant structure–activity relationship (SAR) information and improve inhibitory activity of lead compound **1**, chemical modifications were performed in three cycles. First, we incorporated various steric, electronic, and hydrophobic groups at positions 2, 3, and 6 of the quinoxaline ring in compound **1**, and 22 analogues (**12a–v**) were designed (Table 1). Second, to simplify the structure, by maintaining the 6-nitro-quinoxaline ring, we designed and synthesized 8 monoamino-substituted analogues at 2 or 3 of

Table 1. Chemical Structures of Compounds 1 and 12a–v and Their activities

empd	R ₁	R ₂	Inhibitory rate at 2.5 μM ^a (%)	empd	R ₁	R ₂	Inhibitory rate at 2.5 μM ^a (%)
1	-NO ₂		54	12l	-NO ₂		42
12a	-NO ₂		68	12m	-NO ₂		38
12b	-NO ₂		53	12n	-NO ₂		32
12c	-NO ₂		57	12o	-NO ₂		55
12d	-NO ₂		55	12p	-NO ₂		39
12e	-NO ₂		33	12q	-NO ₂		32
12f	-NO ₂		42	12r	-CF ₃		52
12g	-NO ₂		19	12s	-CF ₃		24
12h	-NO ₂		32	12t	-OCH ₃		23
12i	-NO ₂		31	12u	-NH ₂		50
12j	-NO ₂		72	12v	-NH ₂		41
12k	-NO ₂		54				

^aThe inhibition rate of the exoenzyme C3 transferase(C3) as a positive control compound is 117% at 62.5 nM.

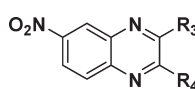
the quinoxaline ring (compounds 13a–h, Table 2) to determine if double amino-substituents on quinoxaline ring are necessary for ligand–enzyme interaction. Finally, 10 compounds 14a–j (Table 3) were prepared to estimate if the type of heterocycles and side-chain substituents on the heterocycle would affect inhibitory activity.

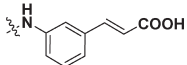
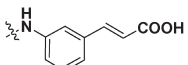
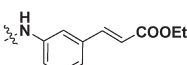
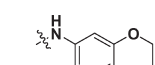
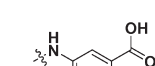
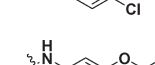
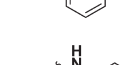
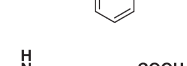
2.2.2. Synthetic Procedures. Scheme 1 depicts the synthetic route for the preparation of compounds 1 and 12a–v. Treatment of 4-substituted-*o*-phenylenediamines 4 with diethyl oxalate 5 in hydrochloric acid solution under reflux quickly afforded quinoxalinediones 6, followed by chlorination with POCl₃ to get

2,3-dichloro-6-substituted quinoxaline 7. Compounds 7 were converted to compounds 1 and 12a–t by S_AR_N2 or C–N coupling under microwave radiation. The catalytic hydrogenation of 6-nitro-quinoxalines 12h and 12j in the presence of 10% Pd/C in MeOH afforded the corresponding 6-aminoquinoxaline derivatives 12u and 12v.

Compounds 13a–h were synthesized through the approach outlined in Scheme 2. Quinoxalin-2-ol 8a was nitrified using HNO₃/AcOH and KNO₃/H₂SO₄ at room temperature to afford 7-nitroquinoxalin-2-ol 9a and 6-nitroquinoxalin-2-ol 9b, respectively, which was converted to the corresponding

Table 2. Chemical Structures of Compounds 13a–h and Their Activities



compd	R ₃	R ₄	Inhibitory rate at 2.5 μM ^a (%)
13a		H	51
13b	H		58
13c		H	66
13d		H	54
13e		H	47
13f		H	40
13g		H	43
13h		H	11

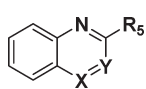
^a The inhibition rate of the exoenzyme C3 transferase(C3) as a positive control compound is 117% at 62.5 nM.

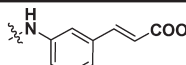
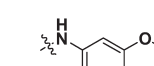
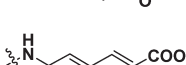
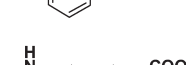
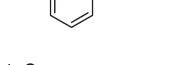
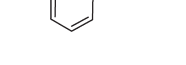
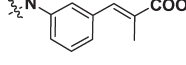
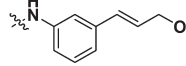
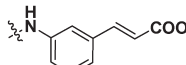
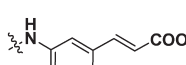
aryl chlorides **10a** and **10b** by refluxing with POCl₃ and PCl₅. Then **10a** and **10b** were substituted by using different aromatic amines, giving the target compounds **13c–d** and **13f–g**, and esters of compounds **13a–b**, **13e**, and **13h**, which were hydrolyzed using LiOH at 25 °C to give carboxylic acid products.

Compounds **14a–j** were synthesized by using a process similar to that for compounds **13a–h** (Scheme 3).

2.3. Biological Assays. **2.3.1. SPR Assay.** Interaction studies between compounds and RhoA were performed with the SPR-based biosensor instrument Biacore 3000 (Biacore AB, Uppsala, Sweden). Each compound was dissolved in dimethyl sulfoxide (DMSO) as a 10 mM stock solution for the Biacore experiments. RhoA was immobilized on the sensor surface by the standard primary amine coupling reaction to the carboxymethylated matrix dextran of a sensor chip CM5 (Biacore AB, Uppsala, Sweden). Equilibration of the baseline was completed by continuous flow of HBS-EP running buffer (10 mM Hepes, 150 mM NaCl, 3 mM EDTA, and 0.005% (v/v) surfactant P₂₀, pH 7.4) through the chip overnight. One of the four serial flow cells was activated for 7 min by injecting a 1:1 fresh mixture of 0.2 M *N*-ethyl-*N'*-dimethylaminopropyl carbodiimide (EDC) and 50 mM *N*-hydroxysuccinimide (NHS) at 25 °C. RhoA was diluted with 10 mM sodium acetate buffer at pH 4.2 to a concentration of 25 μg/mL and immobilized to the surface of sensor chip CM5. Finally, the unreacted protein was blocked by injecting 1 M

Table 3. Chemical Structures of Compounds 14a–j and Their Activities



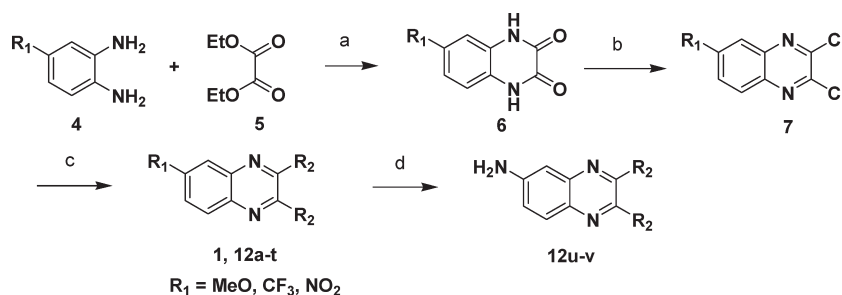
compd	X	Y	R ₅	Inhibitory rate at 2.5 μM ^a (%)
14a	N	C		78
14b	N	C		72
14c	N	C		63
14d	N	C		76
14e	N	C		68
14f	N	C		59
14g	N	C		82
14h	C	C		90
14i	—	NH		48
14j	C	N		47

^a The inhibition rate of the exoenzyme C3 transferase(C3) as a positive control compound is 117% at 62.5 nM.

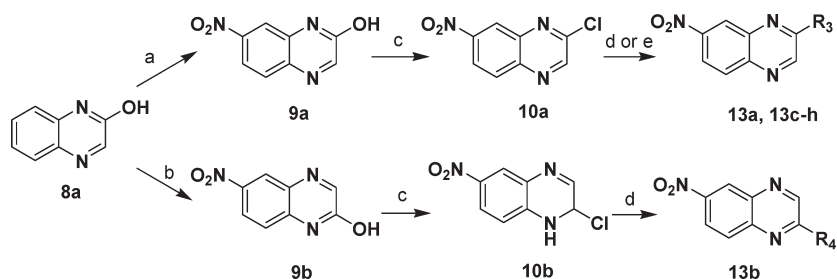
ethanolamine-HCl at pH 8.5 for 7 min, resulting in immobilized densities of 7000 response units (RU). After stabilizing the baseline, Biacore data were collected at 25 °C with HBS-EP (containing 0.4% DMSO) as the running buffer at a constant flow of 30 μL/min. All the sensorgrams were processed by using automatic correction for nonspecific bulk refractive index effects. The equilibrium constants (K_D s) evaluating the protein–inhibitor binding affinity were determined by the 1:1 Langmuir binding fitting model using eq 1. The kinetic analysis of RhoA/inhibitors binding by SPR were described in Supporting Information.

$$K_D = \frac{k_{off}}{k_{on}} \quad (1)$$

where k_{off} represents dissociation rate constant, k_{on} represents the association rate constant.

Scheme 1^a

^a Reagents and conditions: (a) 4N HCl, reflux, 2 h; (b) POCl₃, DMF, reflux, overnight; (c) Cs₂CO₃, dioxane, MW 160 °C, 30 min or Pb(Ph₃P)₄, Cs₂CO₃, MW 160 °C, 30 min; (d) H₂, 10% Pb/C, MeOH, rt, 3 h.

Scheme 2^a

^a Reagents and conditions: (a) HNO₃, AcOH, 25 °C; (b) KNO₃, H₂SO₄, 25 °C; (c) POCl₃, PCl₅, reflux, 4 h; (d) For 13a–b, 13e, and 13 h: (i) DMF, reflux, 2–5 h, (ii) LiOH, MeOH, 25 °C, 2 h; (e) For 13c–d and 13f–g: DMF, reflux, 2–5 h.

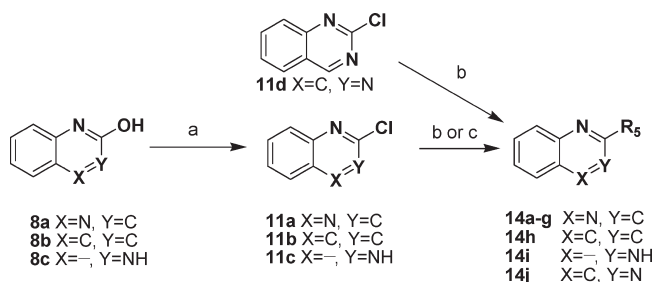
2.3.2. RhoA Activation Assay. When the cell cultures reached 70% confluence (see Experimental Section), the culture media was removed, and the cells were starved overnight in serum-free DMEM (0% fetal bovine serum (FBS)). Then 1.25 μL of compound or DMSO (final concentration of compound, 2.5 μM) was added to the cells. After an additional 1 h of incubation at 37 °C, cells were treated with or without oleoyl-L-α-lysophosphatidic acid (LPA, 5 μg/mL) for 3 min. Following treatment, the culture medium was removed, and the cells were washed in ice-cold PBS and lysed. Thereafter, RhoA activity was measured from the cell lysates using the absorbance-based RhoA G-LISA activation assay biochem kit (Cytoskeleton) according to the manufacturer's protocol. Briefly, cell lysates were isolated using the provided cell lysis buffer and clarified by centrifugation at 10,000 rpm at 4 °C for 2 min before being snap-frozen. Active, GTP-bound, RhoA in cell lysates would bind to the wells to which a Rho-GTP-binding protein was linked but not the inactive GDP-bound RhoA. Active RhoA was detected using indirect immunodetection followed by a colorimetric reaction measured by absorbance at 490 nm. The inhibitory rate (IR) was calculated by using the follow eq 2.

$$IR = \frac{OD_L - OD_C}{OD_L - OD_D} \quad (2)$$

where L represents DMSO + LPA, C represents compound + LPA, and D is DMSO.

2.3.3. Isometric Contraction Measurement. Isometric contraction was measured in rings from the thoracic aortic rings as previously described.³³ Briefly, isolated aortic rings were

mounted between two stainless steel clips in vertical 10-mL organ baths filled with Modified K-H, maintained at 37 °C, and equilibrated with 95% O₂–5% CO₂. The upper stainless steel clip was connected to a force transducer. Isometric tension was recorded by an analogue-to-digital system (ALCB10 MPA2000; Shanghai Alcott Biotech Co. Ltd., China) connected to a desktop computer. The rings were initially placed under the optimal resting tension of 1.5 g and incubated for 90 min until a stable rest tension was achieved, and the solution was changed every 20 min to remove metabolites. The tissues were challenged with a K-rich (80 mM) solution obtained by substituting an equimolar of KCl for NaCl in the Modified K-H repeatedly before the experiment, applied to obtain ring contractions similar in both amplitude and kinetics. A cumulative concentration–response curve to the α₁-agonist PE (10^{−9}–10^{−5} M) was then constructed to determine the concentration of agonist required to produce 70–80% of the maximal contraction (EC_{70–80}). Successful removal of endothelium was confirmed by the inability of acetylcholine (1 μM) to induce relaxation in PE-induced submaximal contraction. After this run-up procedure, the ring was entered into an experimental protocol. The pharmacological effect of the compound was studied on rings submaximally contracted with PE. Once a steady contraction was observed, one aorta ring was treated with the compound (100 mM, dissolved in 100% DMSO) added in a cumulative manner (final concentration was 30 μM–180 μM), whereas another ring of each vessel received only the same volume of solvent (DMSO (3 μL–18 μL)) and was used as a paired time control. The concentration of compound was increased once the maximal relaxant effect of the preceding concentration had been recorded, i.e., after 5 min.

Scheme 3^a

^a Reagents and conditions: (a) POCl₃, PCl₅, reflux, 4 h; (b) For **14a**, **14d–f**, and **14h–j**: (i) DMF, reflux, 2–5 h, (ii) LiOH, MeOH, 25 °C, 2 h; (c) For **14b–c** and **14g**: DMF, reflux, 2–5 h.

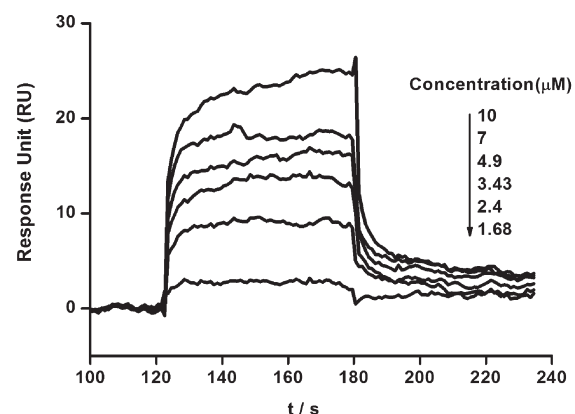
3. RESULTS AND DISCUSSION

3.1. Identification of Binders (Hits) by Virtual Screening.

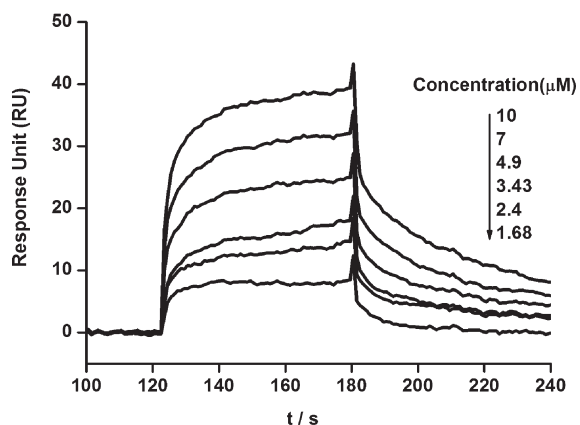
Targeting the crystal structure of RhoA, we searched the SPECS database by molecular docking. Fifty-four candidates available from the vendor were selected after manual observation of the top 3000 ranked hits. Finally, three compounds (**1**, **2**, and **3**) showing a great binding affinity to RhoA were selected according to the binding affinity of compounds to RhoA in vitro using SPR biosensor technology. The binding curves of compounds **1–3** with RhoA are shown in Figure 3. For kinetic analysis on the Biacore 3000 instrument, various concentrations of these three compounds were injected for 120 min at a flow rate of 30 μL/min to allow for interaction with RhoA immobilized on the sensor chip surface. For the RhoA, all these three candidate molecules resulted in a significant and dose-dependent increase in SPR RU and presented characteristic fast-binding and slow-dissociation curves. The concentration series of **1**, **2**, and **3** were fitted by the 1:1 Langmuir binding model in the Biacore3000 evaluation software for binding affinity determination. The collected data indicated that these three compounds can bind to RhoA in vitro and that the dissociation constant (K_D) to RhoA is in the micromolar range ($K_D = 4.47–13.1 \mu\text{M}$). These compounds could be designated as binders (or hits) of RhoA, and their chemical structures and binding affinities are shown in Figure 2. The kinetic data of three binders **1–3** are listed in Table 1S (Supporting Information). The ranks of three hits (compounds **1–3**) identified from the top 3000 docking candidates with Glide are shown in Table 2S (Supporting Information). The Glide GScore for the cocomplexed GNP in the crystal structure of RhoA was also calculated as a reference (Supporting Information, Table 2S).

3.2. Analogue Design and Synthesis. In total, 41 compounds (**1**, **12a–v**, **13a–h**, and **14a–j**) were designed and synthesized, and their chemical structures are shown in Tables 1–3. These compounds were synthesized through the routes outlined in Schemes 1–3, and the details for synthetic procedures and structural characterizations are described in the Experimental Section. All compounds (**1**, **12a–v**, **13a–h**, and **14a–j**) were confirmed to have ≥95% purity (Supporting Information, Table 3S).

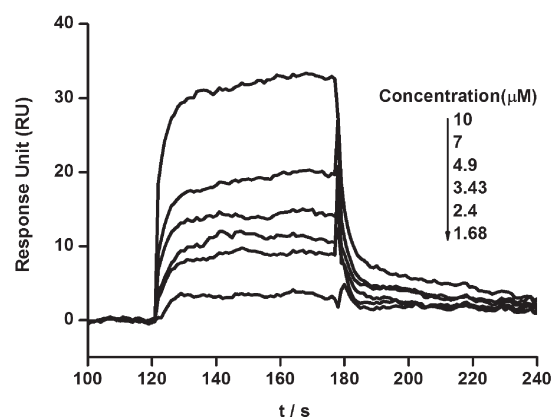
3.3. Biological Activities. **3.3.1. Inhibitory Activity of Compounds 1, 12a–v, 13a–h, and 14a–j.** For the primary assay, using C3 transferase as a positive control, the percent inhibitions of the compounds **1**, **12a–v**, **13a–h**, and **14a–j** at 2.5 μM were measured. The results are summarized in Tables 1–3. Of the



Compound 1



Compound 2



Compound 3

Figure 3. Sensorgrams of compounds **1–3** binding to RhoA measured by SPR. Representative sensorgrams obtained from the injection of compounds **1–3** at concentrations of 1.68, 2.4, 3.43, 4.9, 7.0, and 10.0 μM over RhoA immobilized on the CMS chip.

synthetic derivatives tested, 8 compounds (eg., **12a**, **12j**, **14a–b**, **14d–e**, and **14g–h**) displayed good inhibitory activities against RhoA (expressed as the inhibitory rate at 2.5 μM ≥ 68%), indicating that these are good candidate inhibitors of RhoA. In further studies, we found that the inhibition of RhoA increased in the concentration range from 0 to 10 μM of 8 inhibitors. The curve finally reached steady state in a concentration dependent manner. The half maximal inhibitory concentration (IC_{50})

Table 4. Inhibitory Activities and IC₅₀ Values of the Compounds Tested

compd	inhibitory rate at 2.5 μM ^a (%)	IC ₅₀ ^b (μM)	compd	inhibitory rate at 2.5 μM ^a (%)	IC ₅₀ ^b (μM)
1	54.0	3.28 ± 0.30	14d	76.1	2.05 ± 0.07
12a	68.5	2.58 ± 0.25	14e	68.0	2.62 ± 0.59
12j	72.5	2.09 ± 0.34	14g	81.8	1.68 ± 0.13
14a	78.0	1.51 ± 0.13	14h	90.3	1.24 ± 0.08
14b	71.7	3.00 ± 0.31			

^aThe inhibition rate of the exoenzyme C3 transferase (C3) as a positive control compound is 117% at 62.5 nM. ^bData are the means of three independent experiments.

values, ranging from 1.24 to 3.00 μM (Table 4), were calculated by fitting the dose–response curve using a logistic derivative equation in Origin 7.5. In order to do a direct comparison, the IC₅₀ of lead compound 1 was also given in the same methods (Table 4).

Analyzing the data in Tables 1 and 2, we found that the 2,3-amino- and 6-substituents on the quinoxaline ring markedly affected the inhibitory activities (ranging from 11% to 72%). Encouragingly, the inhibition rate of mono amino-substituted, simplified derivatives 13a–b turned out to be good, 51% and 58%, respectively (Table 2), with little difference and in balance with compound 1 (inhibition rate = 54%). It appeared that only one amino-substituent (regardless of substituted position) was sufficient for the interaction. To our surprise, compound 14a and the non-nitro derivative of compound 13a displayed the highest activity among the compounds probed (78%, Table 3), much more potent than lead compound 1 (inhibition rate = 54%) and analogues 12a–v and 13a–h (inhibition rate ≤ 72%). Furthermore, the most potent derivative 14h (90%, Table 3), replacing the quinoxaline ring with the quinoline ring, was obtained in the whole series. Remarkably, the inhibitory activity of the most potent compound 14h (IC₅₀ = 1.24 ± 0.08 μM, Table 4) increased approximately 3 times than that of lead compound 1 (IC₅₀ = 3.28 ± 0.30 μM, Table 4), demonstrating that the chemical modification strategy employed in this study is efficient and valuable for further structural modification.

3.3.2. Effect of Compounds 14g–h against PE-Induced Contraction in Thoracic Aorta Artery Rings. To test the vasorelaxation effects of the inhibitors against PE-induced contraction in thoracic aorta artery rings, two of the most potent inhibitors of RhoA (14g and 14h) have been evaluated. In all vessels submaximally contracted with 100 nM PE (produce 70–80% of the maximal contraction), compounds 14g–h (0–180 μM) strongly inhibited the tension development in a dose dependent fashion (Figure 4). The maximal inhibitions of compounds 14g and 14h were 78.57 ± 2.47% and 55.92 ± 4.01%, respectively (180 μM, Figure 4). The IC₅₀ values of compounds 14g and 14h were 135.9 μM and 161.3 μM, respectively. These results indicated that compounds 14g–h showed partial influence on the PE-induced contraction in thoracic aorta artery rings and were good leads for designing more potent cardiovascular drugs.

3.4. SAR. The SAR analysis of a set of 41 compounds provided important insights of the essential structural requirements for effective RhoA inhibition. An analysis of the data shown in Tables 1–3 reveals some noteworthy observations of the SAR for compounds 1, 12a–v, 13a–h, and 14a–j: (1) mono as well as double amino-substituents on the quinoxaline ring can both display high activities (1 vs 13a or 13b). The substituent effect is limited; (2) the displacement of –NO₂ on the quinoxaline ring with –CF₃ (12a vs 12r and 12b vs 12s), –OMe (12b vs 12t),

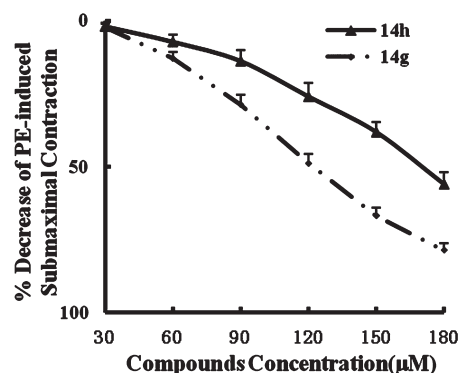


Figure 4. Effect of increasing concentration of 14h and DMSO on PE-induced submaximal contraction in isolated arterial rings. Values are the means ± SE (**P* < 0.01 ANOVA *n* = 6).

and –NH₂ (12j vs 12v) is not beneficial; (3) 6-nitro substitutions on the monoamino quinoxaline ring substantially decreases the inhibitory activity of the derivatives (14a vs 13a, 14d vs 13h, and 14b vs 13d); (4) among the quinoxaline (14a), quinoline (14h), benzimidazole (14i), and quinazoline (14j) frameworks, the quinoline ring is optimal and significantly improves the biological activities. Taken together, the SARs are mixed. A subtle interplay between heterocyclic scaffolds, steric effects, polarity, and hydrogen-bonding capability seemed to be critical for high potency. Compounds 14g and 14h represented seemingly the best combination.

3.5. Binding Models. To understand the structural basis for the binding affinities of the inhibitors for RhoA, we scrutinized the binding poses of hit compound 1 and the most potent derivative 14h by means of molecular docking. Figure 5 shows the predicted binding poses of 1 (Figure 5B) and 14h (Figure 5C) in the GNP-binding site. The binding mode of the cocomplexed GNP of RhoA is shown in Figure 5A, which is featured by the triphosphate chelating the magnesium cation and guanine moiety anchored by Asp120 and Lys162. The triphosphate group and the ribose ring also form complex hydrogen bonds with the backbone of the surrounding residues as well as salt bridge with Lys18, which further stabilized the binding pose of GNP. For hit 1, the quinoxaline moiety acts as a bridge between the pair of acrylic acid groups, which extend to the two anchor binding sites occupied by the guanine and triphosphate groups, respectively, in GNP. The acrylic acid groups can be regarded as the payload and form strong salt bridges with the basic residues such as Lys18 and Lys118. Moreover, one of the carboxylates can coordinate with the magnesium cation (Figure 5B). Although the anchor points mentioned above contribute remarkably to the binding affinity of compound 1, the hydrophobic quinoxaline moiety is predicted to

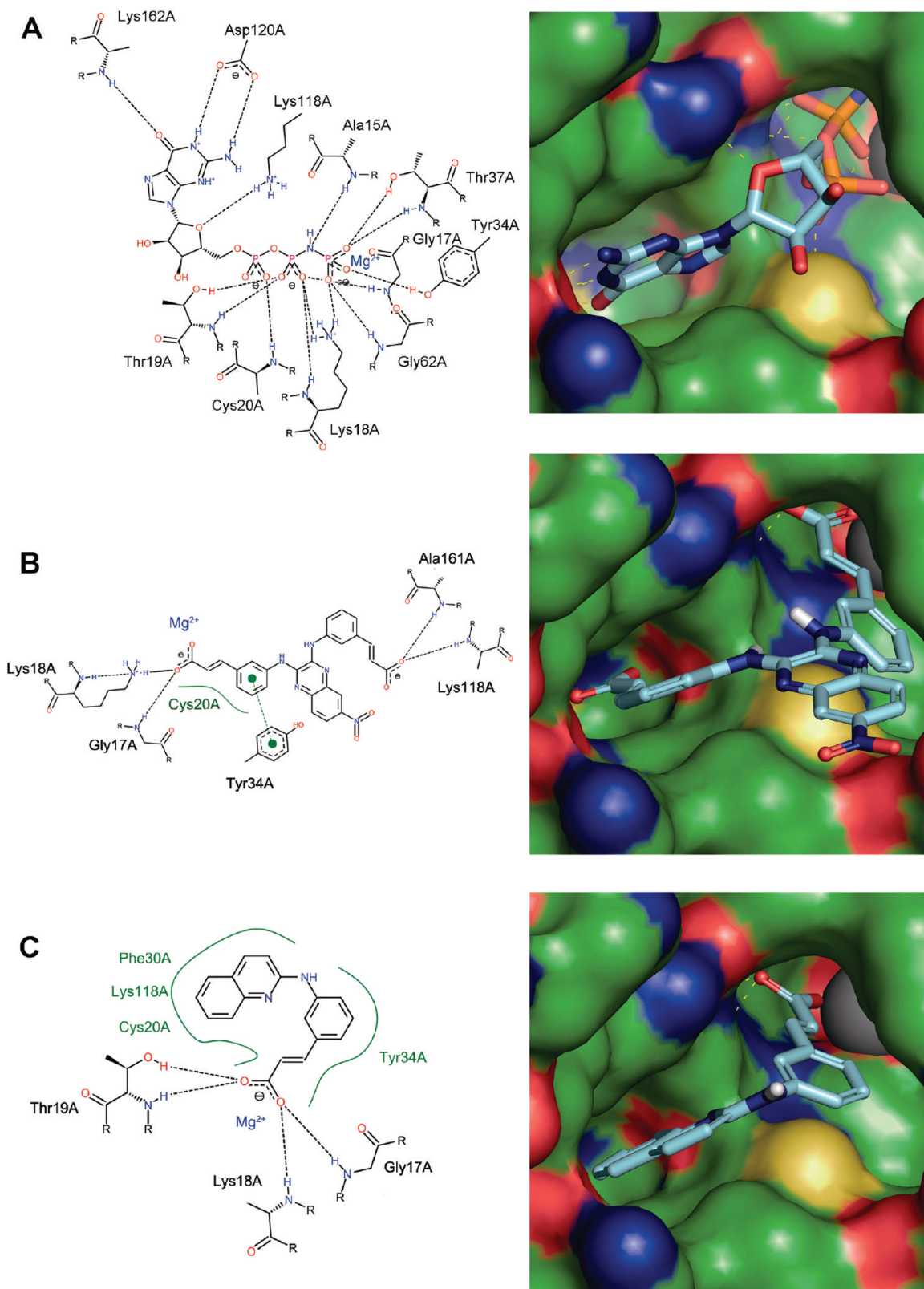


Figure 5. Two-dimensional (2D) and three-dimensional (3D) interaction schemes of cocomplexed GNP (A) of RhoA and docked poses of **1** (B) and **14h** (C) in the GNP-binding site of RhoA. The figures were prepared using PoseViewWeb (<http://poseview.zbh.uni-hamburg.de/poseview>) and PyMol (<http://pymol.sourceforge.net/>). The ligands are shown as sticks, and the noncarbon atoms are colored by atom types (receptor carbon in green and ligand carbon in cyan). The magnesium ion in the phosphate binding site was rendered as gray spheres. Critical residues of the binding pocket are labeled in the 2D interaction views. Hydrogen bonds are shown as dotted lines in both 2D and 3D views.

be completely exposed to the solvent, rendering the binding pose extremely unstable with respect to the remarkable entropy penalty, which may explain its moderate inhibitory activity against RhoA. Moreover, the gain of the binding affinity from the hydrogen bonds between the carboxylate group and residues in the guanine site such as Lys118 and Ala161 may be offset by the electrostatic repellency with the nearby negatively charged residue Asp120. The binding affinity for compound **1** with Glide GScore also justifies the binding preference over the GNP (as shown in Table 2S, Supporting Information) in the same binding site and most likely in a competitive way. For compound **14h**, the carboxylate can also form the hydrogen bond networks and other strong interactions observed in the case of **1**. The quinoline ring occupies the guanine binding site and results in a visible burying in the hydrophobic sandwiches consisting of Cys20, Phe30, and Lys118 (Figure 5C), which may compensate the binding affinity loss brought by truncation of the acrylic acid group in **1**. The bottom of the guanine binding site is spatially constrained and relatively hydrophobic, and cannot accommodate larger polar groups such as nitro, which attributes to the lower inhibitory activity of **13a** and **13h** compared with that of their counterparts without the nitro groups such as **14a** and **14d**.

4. CONCLUSIONS

In summary, we have discovered first-in-class small molecular RhoA inhibitors by using a structure-based virtual screening approach in conjunction with chemical synthesis and bioassays. On the basis of the structure of lead compound **1**, chemical modifications were performed in three cycles. In total, 41 new compounds have been synthesized and tested with biological assays. Finally, eight compounds (**12a**, **12j**, **14a–b**, **14d–e**, and **14g–4h**) were found to show high RhoA inhibition activities, and two compounds (**14g** and **14h**) showed significant inhibitory effects against PE-induced contraction in thoracic aorta artery rings. Molecular binding models give rational explanations about SARs, which are in good agreement with pharmacological results. Notably, to our knowledge, compounds **14g** and **14h** with IC₅₀ values of 1.68 μM and 1.24 μM against RhoA activation and IC₅₀ values of 135.9 μM and 161.3 μM to the relaxation of PE-induced contraction are the most potent small molecular RhoA inhibitors reported up to date, which are likely to be developed into new promising agents for cardiovascular diseases and are currently being pursued in our laboratories.

5. EXPERIMENTAL SECTION

5.1. General. **5.1.1. Chemistry.** The reagents (chemicals) were purchased from Lancaster, Alfa Aesar, J&K, Acros, and Shanghai Chemical Reagent Co. and used without further purification. Analytical thin-layer chromatography (TLC) was performed on HSGF 254 (150–200 μm thickness; Yantai Huiyou Co., China). Yields were not optimized. Melting points were measured in a capillary tube on a SGW X-4 melting point apparatus without correction. Nuclear magnetic resonance (NMR) spectroscopy was performed on Bruker AMX-500, AMX-400, and AMX-300 NMR (IS as TMS). Chemical shifts were reported in parts per million (ppm, δ) downfield from tetramethylsilane. Proton coupling patterns were described as singlet (s), doublet (d), triplet (t), quartet (q), multiplet (m), and broad (br). Low- and high-resolution mass spectra (LRMS and HRMS) were given with electric, electrospray, and matrix-assisted laser desorption ionization (EI, ESI, and MALDI) produced by a Finnigan MAT-95, LCQ-DECA spectrometer and IonSpec 4.7 T. Compounds **1**, **12a–v**, **13a–h**, and **14a–j** were confirmed ≥95% purity (Supporting

Information, Table 3S). The details for purity analyses of compounds **1**, **12a–v**, **13a–h**, and **14a–j** are described in the Supporting Information.

5.1.2. Biology. All solvents and reagents with reagent grade or ultrapure quality were purchased commercially and were used without further purification. The vector pRSET B and DMEM and FBS were purchased from Invitrogen. The bacterial strain *E. coli* strain BL21 was purchased from Qiagen. The chelating column and protein molecular weight marker for SDS–PAGE were from Amersham Pharmacia Biotech. Amicon Ultra-4 centrifugal filter devices were purchased from Millipore. The Human brain vascular smooth muscle cells were purchased from ScienCell. The PE, LPA, and DMSO were purchased from Sigma. The RhoA G-LISA activation assay biochem kit and C3 transferase were purchased from Cytoskeleton.

5.1.2.1. 6-Nitro Quinoxaline-2,3(1H,4H)-dione (6a). Representative Procedure for 6a–6c. 4-Nitrobenzene-1,2-diamine (15.3 g, 0.1 mol) and diethyl oxalate (0.15 mol) were added slowly to 40 mL of 4 M HCl. After stirring for 5 min at room temperature, the reaction mixture was heated to reflux for 2 h. Then the reaction mixture was moved to room temperature for 10 min, the deposited crystals were obtained by filtration and washed with water. Yield: 85%. ¹H NMR (400 MHz, DMSO-*d*₆) δ: 7.21 (d, *J* = 8.8 Hz, 1H), 7.90–7.95 (m, 2H), 12.16 (s, 1H), 12.35 (s, 1H). LC-MS *m/z* 208 [M + H]⁺.

5.1.2.2. 6-Trifluoromethyl Quinoxaline-2,3(1H,4H)-dione (6b). In the same manner as that described for the preparation of **6a**, **6b** was prepared from 4-trifluoromethylbenzene-1,2-diamine and diethyl oxalate. Yield: 82%. LC-MS *m/z* 231 [M + H]⁺.

5.1.2.3. 6-Methoxy Quinoxaline-2,3(1H,4H)-dione (6c). In the same manner as that described for the preparation of **6a**, **6c** was prepared from 4-methoxybenzene-1,2-diamine and diethyl oxalate. Yield: 83%. LC-MS *m/z* 192 [M + H]⁺.

5.1.2.4. 2,3-Dichloro-6-nitroquinoxaline (7a). Representative Procedure for 7a–7c. 6-Nitro quinoxaline-2,3(1H,4H)-dione **6a** (0.1 mol) was slowly added to POCl₃ (30 mL), and then *N,N*-dimethylformamide (DMF, 0.5 mL) was added. The reaction mixture was heated under reflux and kept overnight. After being cooled to about 20 °C, it was poured into 300 mL of ice water. The solid thus separated as shining needles, was filtered, and washed with ice water to give **7a** as a gray solid. Yield: 90%. ¹H NMR (400 MHz, DMSO-*d*₆) δ: 8.19 (dd, *J*₁ = 8.8 Hz, *J*₂ = 16 Hz, 1H), 8.29 (d, *J* = 8.8 Hz, 1H), 8.52 (s, 1H). LC-MS *m/z* 245 [M + H]⁺.

5.1.2.5. 2,3-Dichloro-6-trifluoromethyl Quinoxaline (7b). In the same manner as that described for the preparation of **7a**, **7b** was prepared from 6-trifluoromethyl quinoxaline-2,3(1H,4H)-dione (**6b**) and POCl₃. Yield: 85%. LC-MS *m/z* 268 [M + H]⁺.

5.1.2.6. 2,3-Dichloro-6-methoxy Quinoxaline (7c). In the same manner as that described for the preparation of **7a**, **7c** was prepared from 6-methoxy quinoxaline-2,3(1H,4H)-dione (**6c**) and POCl₃. Yield: 81%. LC-MS *m/z* 230 [M + H]⁺.

5.1.2.7. (2*E*,2'*E*)-3,3'-(3,3'-(6-Nitroquinoxaline-2,3-diyl)bis(azanediyl)bis(3,1-phenylene)diacrylic Acid (1). 2,3-Dichloro-6-nitroquinoxaline (**5a**, 0.01 mol), (*E*)-ethyl 3-(3-aminophenyl) acrylate (0.05 mol), Pb(Ph₃P)₄ (0.003 mol), and Cs₂CO₃ (0.05 mol) were added to a solution of dioxane (5 mL) in a vial. The reaction mixture was then irradiated for 30 min at 160 °C. After the reaction was cooled to ambient temperature, it was poured into water and extracted with dichloromethane (DCM) three times, and the combined organic layer was washed, dried over MgSO₄, filtered, and concentrated in vacuo and then purified by chromatography with EtOAc/petroleum ether to give the precursor of product, which was then hydrolyzed with 10% NaOH. After the reaction was completed, positive ion-exchange resin (Dowex 50w X 4-400) was added to the reaction mixture to neutralize the excess base, filtered, and concentrated in vacuo to give **1** as a yellow solid. Yield: 35%; mp >300 °C. ¹H NMR (500 MHz, DMSO-*d*₆) δ: 6.51 (d, *J* = 16.0 Hz, 2H), 7.49–7.51 (m, 4H), 7.60–7.70 (m, 3H), 7.95–8.04 (m, 2H),

8.12–8.23 (m, 3H), 8.43 (s, 1H), 9.50 (s, 1H), 9.65 (s, 1H); HRMS (ESI) m/z calcd $C_{26}H_{20}N_2O_6$ [$M + H$]⁺ 498.1414; found, 498.1406.

5.1.2.8. (2*E*,2'*E*)-3,3'-(3,3'-(6-Nitroquinoxaline-2,3-diyl)bis(azanediyl)bis(4,1-phenylene)diacrylic Acid (**12a**). In the same manner as that described for the preparation of **1**, **12a** was prepared from 2,3-dichloro-6-nitroquinoxaline (**5a**) and (*E*)-ethyl 3-(4-aminophenyl) acrylate. Yield: 25%; mp >300 °C. ¹H NMR (300 MHz, DMSO-*d*₆) δ: 6.46 (dd, $J_1 = 15.3$ Hz, $J_2 = 3.6$ Hz, 2H), 7.53–7.72 (m, 7H), 8.10–8.18 (m, 5H), 8.33 (d, $J = 2.4$ Hz, 1H). ESI-MS m/z 495.9 [$M - H$][−]; HRMS (ESI) m/z calcd $C_{26}H_{18}N_2O_6$ [$M - H$][−] 496.1257; found, 496.1262.

5.1.2.9. (2*E*,2'*E*)-Diethyl 3,3'-(((6-nitroquinoxaline-2,3-diyl)bis(azanediyl)bis(4,1-phenylene)diacrylate (**12b**). In the same manner as that described for the preparation of **1**, **12b** was prepared from 2,3-dichloro-6-nitroquinoxaline (**5a**) and (*E*)-ethyl 3-(4-aminophenyl) acrylate. Yield: 30%; mp 212 °C. ¹H NMR (300 MHz, DMSO-*d*₆) δ: 1.27 (t, $J = 7.5$ Hz, 6H), 4.20 (q, $J = 7.5$ Hz, 4H), 6.52–6.60 (m, 2H), 7.62–7.79 (m, 7H), 8.80–8.14 (m, 4H), 8.13 (d, $J = 9$ Hz, 1H), 8.34 (s, 1H), 9.63 (br, 1H), 9.77 (br, 1H); EI-MS m/z 553 (M^+). HRMS (EI) m/z calcd for M^+ 553.1961; found, 553.1946.

5.1.2.10. 2,3-Bis(4-(2-fluorophenyl)piperidin-1-yl)-6-nitroquinoxaline (**12c**). 2,3-Dichloro-6-nitroquinoxaline (**5a**, 0.01 mol), 1-(2-fluorophenyl)piperazine (0.05 mol), and Cs_2CO_3 (0.05 mol) were added to a solution of dioxane (5 mL) in the vial. The reaction mixture was then irradiated for 30 min at 160 °C. After the reaction was cooled to ambient temperature, it was poured into water and extracted with DCM three times, and the combined organic layer was washed, dried over $MgSO_4$, filtered, and concentrated in vacuo and then purified by chromatography with DCM/MeOH to give **12c** as a yellow solid. Yield: 80%. mp 189 °C. ¹H NMR (300 MHz, $CDCl_3$) δ: 3.28 (br, 8H), 3.82 (br, 4H), 3.93 (br, 4H), 6.98–7.04 (m, 8H), 7.76 (d, $J = 9$ Hz, 1H), 8.22 (dd, $J_1 = 9.3$ Hz, $J_2 = 2.4$ Hz, 1H), 8.62 (d, $J = 2.4$ Hz, 1H); EI-MS m/z 531 (M^+). HRMS (EI) m/z calcd for M^+ 531.2194; found, 531.2194.

5.1.2.11. 2,3-Bis(4-(benzo[d][1,3]dioxol-5-yl)piperazin-1-yl)-6-nitroquinoxaline (**12d**). In the same manner as that described for the preparation of **12c**, **12d** was prepared from 2,3-dichloro-6-nitroquinoxaline (**5a**) and 1-(benzo[d][1,3]dioxol-5-yl)piperazine. Yield: 75%. mp 93 °C. ¹H NMR (300 MHz, $CDCl_3$) δ: 2.57 (br, 8H), 3.58 (s, 4H), 3.69 (s, 4H), 5.96 (s, 4H), 6.77 (s, 4H), 6.89 (s, 2H), 7.67 (d, $J = 6.3$ Hz, 1H), 8.16 (dd, $J_1 = 9$ Hz, $J_2 = 2.7$ Hz, 1H), 8.54 (d, $J = 2.7$ Hz, 1H); EI-MS m/z 583 (M^+). HRMS (EI) m/z calcd for M^+ 583.2179; found, 583.2183.

5.1.2.12. 8-(3-{1,4-Dioxo-8-azaspiro[4.5]decan-8-yl}-7-nitroquinoxalin-2-yl)-1,4-dioxo-8-azaspiro[4.5]decan-8-yl (**12e**). In the same manner as that described for the preparation of **12c**, **12e** was prepared from 2,3-dichloro-6-nitroquinoxaline (**5a**) and 1,4-dioxo-8-azaspiro[4.5]decan-8-yl. Yield: 88%. mp 182–183 °C. ¹H NMR (300 MHz, $CDCl_3$) δ: 1.86 (br, 8H), 3.70 (br, 4H), 3.83 (br, 4H), 4.01 (s, 8H), 7.68 (d, $J = 9$ Hz, 1H), 8.16 (dd, $J_1 = 9$ Hz, $J_2 = 2.7$ Hz, 1H), 8.54 (d, $J = 2.7$ Hz, 1H); EI-MS m/z 457 (M^+). HRMS (EI) m/z calcd for M^+ 457.1961; found, 457.1966.

5.1.2.13. Diethyl 1,1'-(6-nitroquinoxaline-2,3-diyl)bis(piperidine-3-carboxylate) (**12f**). In the same manner as that described for the preparation of **12c**, **12f** was prepared from 2,3-dichloro-6-nitroquinoxaline (**5a**) and ethyl piperidine-3-carboxylate. Yield: 81%. mp <50 °C. ¹H NMR (300 MHz, $CDCl_3$) δ: 1.24–1.31 (m, 6H), 1.61–2.11 (m, 8H), 2.66–3.22 (m, 6H), 3.96–4.29 (m, 6H), 4.33–4.53 (m, 2H), 7.70 (dd, $J_1 = 9$ Hz, $J_2 = 1.5$ Hz, 1H), 8.17 (dd, $J_1 = 9$ Hz, $J_2 = 2.4$ Hz, 1H), 8.55–8.57 (m, 1H); EI-MS m/z 485 (M^+). HRMS (EI) m/z calcd for M^+ 485.2274; found, 485.2262.

5.1.2.14. 1,1'-(6-Nitroquinoxaline-2,3-diyl)bis(piperidine-3-carboxylic Acid) (**12g**). Diethyl 1,1'-(6-nitroquinoxaline-2,3-diyl)bis(piperidine-3-carboxylate) (**12f**) was hydrolyzed with 10% NaOH in MeOH. After the reaction was completed, positive ion-exchange resin (Dowex 50w X 4–400) was added to the reaction mixture to neutralize the excess base, filtered, and concentrated in vacuo to give **12g** as a

yellow solid. Yield: 83%. mp 135 °C. ¹H NMR (400 MHz, DMSO-*d*₆) δ: 1.49–1.69 (m, 4H), 1.79–1.99 (m, 4H), 2.57–3.13 (m, 5H), 3.86–4.33 (m, 4H), 7.68–7.72 (m, 1H), 8.10–8.14 (m, 1H), 8.33–8.35 (m, 1H); EI-MS m/z 429 (M^+). HRMS (EI) m/z calcd for M^+ 429.1648; found, 429.1656.

5.1.2.15. Diethyl 1,1'-(6-nitroquinoxaline-2,3-diyl)bis(piperidine-4-carboxylate) (**12h**). In the same manner as that described for the preparation of **12c**, **12h** was prepared from 2,3-dichloro-6-nitroquinoxaline (**5a**) and ethyl piperidine-4-carboxylate. Yield: 89%. mp 97 °C. ¹H NMR (300 MHz, $CDCl_3$) δ: 1.28 (t, $J = 7.2$ Hz, 6H), 1.80–1.91 (m, 4H), 2.06–2.12 (m, 4H), 2.53–2.58 (m, 2H), 2.88–3.04 (m, 4H), 4.14–4.21 (q, $J = 7.2$ Hz, 4H), 4.21–4.25 (m, 4H), 4.38–4.43 (m, 4H), 7.69 (d, $J = 9$ Hz, 1H), 8.16 (dd, $J_1 = 9$ Hz, $J_2 = 2.4$ Hz, 1H), 8.55 (d, $J = 2.4$ Hz, 1H); EI-MS m/z 485 (M^+). HRMS (EI) m/z calcd for M^+ 485.2274; found, 485.2275.

5.1.2.16. Dimethyl 1,1'-(6-nitroquinoxaline-2,3-diyl)bis(piperidine-4-carboxylate) (**12i**). In the same manner as that described for the preparation of **12c**, **12i** was prepared from 2,3-dichloro-6-nitroquinoxaline (**5a**) and methyl piperidine-4-carboxylate. Yield: 87%. mp 141 °C. ¹H NMR (300 MHz, $CDCl_3$) δ: 1.82–1.93 (m, 4H), 2.10 (m, 4H), 2.57–2.60 (m, 2H), 2.89–3.07 (m, 4H), 3.73 (s, 6H), 4.24 (d, $J = 13.5$ Hz, 2H), 4.42 (d, $J = 13.5$ Hz, 2H), 7.73 (d, $J = 9.3$ Hz, 1H), 8.18 (d, $J = 9.3$ Hz, 1H), 8.56 (s, 1H); EI-MS m/z 457 (M^+). HRMS (EI) m/z calcd for M^+ 457.1961; found, 457.1955.

5.1.2.17. 1,1'-(6-Nitroquinoxaline-2,3-diyl)bis(piperidine-4-carboxylic acid) (**12j**). Dimethyl 1,1'-(6-nitroquinoxaline-2,3-diyl)bis(piperidine-4-carboxylate) (**12i**) was hydrolyzed with 10% NaOH in MeOH. After the reaction was completed, positive ion-exchange resin (Dowex 50w X 4–400) was added to the reaction mixture to neutralize the excess base, filtered, and concentrated in vacuo to give **12j** as a white solid. Yield: 81%. mp >300 °C. ¹H NMR (400 MHz, $CDCl_3$) δ: 1.63–1.73 (m, 4H), 1.97–2.00 (m, 4H), 2.87–3.02 (m, 4H), 3.40–3.49 (m, 1H), 4.14 (d, $J = 12.8$ Hz, 2H), 4.33 (d, $J = 12.8$ Hz, 2H), 7.67 (d, $J = 9.2$ Hz, 1H), 8.11 (dd, $J_1 = 9.2$ Hz, $J_2 = 2.8$ Hz, 1H), 8.31 (d, $J = 2.8$ Hz, 1H), 12.34 (br, 2H); EI-MS m/z 429 (M^+). HRMS (EI) m/z calcd for M^+ 429.1648; found, 429.1646.

5.1.2.18. 4,4'-(6-Nitroquinoxaline-2,3-diyl)dimorpholine (**12k**). In the same manner as that described for the preparation of **12c**, **12k** was prepared from 2,3-dichloro-6-nitroquinoxaline (**5a**) and morpholine. Yield: 92%. mp 180 °C. ¹H NMR (300 MHz, $CDCl_3$) δ: 3.60–3.63 (m, 4H), 3.70–3.74 (m, 4H), 3.85–3.89 (m, 8H), 7.74 (d, $J = 9.3$ Hz, 1H), 8.22 (dd, $J_1 = 9.3$ Hz, $J_2 = 2.4$ Hz, 1H), 8.60 (d, $J = 2.7$ Hz, 1H); EI-MS m/z 345 (M^+). HRMS (EI) m/z calcd for M^+ 345.1437; found, 345.1437.

5.1.2.19. 2,3-Bis(4-methylpiperidin-1-yl)-6-nitroquinoxaline (**12l**). In the same manner as that described for the preparation of **12c**, **12l** was prepared from 2,3-dichloro-6-nitroquinoxaline (**5a**) and 4-methylpiperidine. Yield: 89%. mp 159–161 °C. ¹H NMR (300 MHz, $CDCl_3$) δ: 0.99 (s, 3H), 1.01 (s, 3H), 1.25–1.39 (m, 5H), 1.68–1.86 (m, 3H), 1.80 (d, $J = 12.3$ Hz, 2H), 2.78 (dd, $J_1 = 27$ Hz, $J_2 = 13.2$ Hz, 4H), 4.27 (d, $J = 12.6$ Hz, 2H), 4.49 (d, $J = 12.6$ Hz, 2H), 7.62 (d, $J = 8.7$ Hz, 1H), 8.12 (dd, $J_1 = 8.7$ Hz, $J_2 = 3$ Hz, 1H), 8.51 (d, $J = 2.7$ Hz, 1H); EI-MS m/z 369 (M^+). HRMS (EI) m/z calcd for M^+ 369.2165; found, 369.2166.

5.1.2.20. 2,3-Bis(4-(2,4-difluorophenyl)piperazin-1-yl)-6-nitroquinoxaline (**12m**). In the same manner as that described for the preparation of **12c**, **12m** was prepared from 2,3-dichloro-6-nitroquinoxaline (**5a**) and 1-(2,4-difluorophenyl)piperazine. Yield: 75%. mp 213–214 °C. ¹H NMR (300 MHz, $CDCl_3$) δ: 3.22 (br, 8H), 3.81 (br, 4H), 3.91 (br, 4H), 6.80–6.97 (m, 6H), 7.75 (d, $J = 8.7$ Hz, 1H), 8.21 (dd, $J_1 = 9$ Hz, $J_2 = 3$ Hz, 1H), 8.60 (d, $J = 2.4$ Hz, 1H); EI-MS m/z 567 (M^+). HRMS (EI) m/z calcd for M^+ 567.2006; found, 567.1997.

5.1.2.21. N^2,N^3 -Bis(3,4-dimethoxyphenethyl)-6-nitroquinoxaline-2,3-diamine (**12n**). In the same manner as that described for the preparation of **12c**, **12n** was prepared from 2,3-dichloro-6-nitroquinoxaline (**5a**) and 2-(3,4-dimethoxyphenyl)ethanamine. Yield: 71%. mp

136–137 °C. ^1H NMR (300 MHz, CDCl_3) δ : 2.93 (t, $J = 6.9$ Hz, 4H), 3.78–3.86 (m, 16H), 6.72–6.81 (m, 6H), 7.61 (d, $J = 9$ Hz, 1H), 8.10 (dd, $J_1 = 9$ Hz, $J_2 = 2.4$ Hz, 1H), 8.49 (d, $J = 2.7$ Hz, 1H); EI-MS m/z 533 (M^+). HRMS (EI) m/z calcd for M^+ 533.2274; found, 533.228.

5.1.2.22. *6-Nitro- N^2,N^3 -bis(pyridin-4-ylmethyl)quinoxaline-2,3-diamine (12o)*. In the same manner as that described for the preparation of **12c**, **12o** was prepared from 2,3-dichloro-6-nitroquinoxaline (**5a**) and pyridin-4-yl-methanamine. Yield: 61%. mp 207–208 °C. ^1H NMR (300 MHz, $\text{DMSO}-d_6$) δ : 4.79 (dd, $J_1 = 8.4$ Hz, $J_2 = 2.1$ Hz, 4H), 7.42–7.48 (m, 5H), 7.95 (dd, $J_1 = 8.4$ Hz, $J_2 = 2.4$ Hz, 1H), 8.11 (d, $J = 2.7$ Hz, 1H), 8.52–8.56 (m, 5H); EI-MS m/z 387 (M^+). HRMS (EI) m/z calcd for M^+ 387.1444; found, 387.1443.

5.1.2.23. *$N^1,N^{1'}$ -(6-Nitroquinoxaline-2,3-diyl)bis(N^2,N^2 -diethylethane-1,2-diamine) (12p)*. In the same manner as that described for the preparation of **12c**, **12p** was prepared from 2,3-dichloro-6-nitroquinoxaline (**5a**) and N^1,N^1 -diethylethane-1,2-diamine. Yield: 81%. mp 161–163 °C. ^1H NMR (300 MHz, $\text{DMSO}-d_6$) δ : 1.05–1.12 (m, 12H), 2.80–2.94 (br, 12H), 3.66 (br, 4H), 7.48 (d, $J = 9.2$ Hz, 1H), 7.98 (dd, $J_1 = 9$ Hz, $J_2 = 2.7$ Hz, 1H), 8.15 (d, $J = 2.7$ Hz, 1H); EI-MS m/z 403 (M^+). HRMS (EI) m/z calcd for M^+ 403.2696; found, 403.2701.

5.1.2.24. *N^2,N^3 -Bis(4-methylbenzyl)-6-nitroquinoxaline-2,3-diamine (12q)*. In the same manner as that described for the preparation of **12c**, **12q** was prepared from 2,3-dichloro-6-nitroquinoxaline (**5a**) and *p*-tolylmethanamine. Yield: 83%. mp 210–212 °C. ^1H NMR (400 MHz, $\text{DMSO}-d_6$) δ : 2.26 (s, 6H), 4.66 (dd, $J_1 = 12.4$ Hz, $J_2 = 4.8$ Hz, 4H), 7.14 (d, $J = 7.6$ Hz, 4H), 7.27–7.30 (m, 4H), 7.49 (d, $J = 9.2$ Hz, 1H), 7.96 (dd, $J_1 = 8.8$ Hz, $J_2 = 2.4$ Hz, 1H), 8.14 (d, $J = 2.1$ Hz, 1H); EI-MS m/z 413 (M^+). HRMS (EI) m/z calcd for M^+ 413.1852; found, 413.1856.

5.1.2.25. *(2*E*,2'*E*)-3,3'-((6-(Trifluoromethyl)quinoxaline-2,3-diyl)bis(azanediyl))bis(4,1-phenylene)diacrylic Acid (12r)*. In the same manner as that described for the preparation of **1**, **12r** was prepared from 2,3-dichloro-6-nitroquinoxaline (**5a**) and (*E*)-ethyl 3-(4-aminophenyl)acrylate. Yield: 35%. mp 155–157 °C. ^1H NMR (300 MHz, $\text{DMSO}-d_6$) δ : 6.44–6.49 (m, 2H), 7.57–7.62 (m, 4H), 7.67–7.75 (m, 4), 7.89–7.90 (m, 1H), 8.03–8.05 (m, 4H), 9.70–9.74 (m, 2H); ESI-MS m/z 518.9 [$\text{M}-\text{H}$] $^-$. HRMS (ESI) m/z calcd for [$\text{M} - \text{H}$] $^-$ 519.1280; found, 519.1271.

5.1.2.26. *(2*E*,2'*E*)-Diethyl 3,3'-((6-(trifluoromethyl)quinoxaline-2,3-diyl)bis(azanediyl))bis(4,1-phenylene) Diacrylate (12s)*. In the same manner as that described for the preparation of **1**, **12s** was prepared from 2,3-dichloro-6-trifluoromethylquinoxaline (**5a**) and (*E*)-ethyl 3-(4-aminophenyl)acrylate. Yield: 35%. mp 193–194 °C. ^1H NMR (300 MHz, $\text{DMSO}-d_6$) δ : 1.27 (t, $J = 6.9$ Hz, 6H), 4.19 (q, $J = 7.2$ Hz, 4H), 6.52–6.59 (m, 2H), 7.61–7.68 (m, 4H), 7.73–7.9 (m, 4H), 7.97–8.00 (m, 4H), 9.50 (d, $J = 15.6$ Hz, 2H); EI-MS m/z 576 (M^+). HRMS (EI) m/z calcd for M^+ 576.1984; found, 576.1985.

5.1.2.27. *(2*E*,2'*E*)-Diethyl 3,3'-((6-methoxyquinoxaline-2,3-diyl)bis(azanediyl))bis(4,1-phenylene)diacrylate (12t)*. In the same manner as that described for the preparation of **1**, **12t** was prepared from 2,3-dichloro-6-methoxyquinoxaline (**5a**) and (*E*)-ethyl 3-(4-aminophenyl)acrylate. Yield: 37%. mp 103–105 °C. ^1H NMR (300 MHz, $\text{DMSO}-d_6$) δ : 1.26 (t, $J = 6.6$ Hz, 6H), 4.19 (dd, $J_1 = 6.9$ Hz, $J_2 = 1.2$ Hz, 4H), 6.54 (dd, $J_1 = 15.6$ Hz, $J_2 = 6.9$ Hz, 2H), 7.08 (s, 2H), 7.54 (d, $J = 8.7$ Hz, 1H), 7.52–7.62 (m, 1H), 7.66–7.77 (m, 4H), 7.89–7.99 (m, 4H), 9.17 (br, 1H), 9.27 (br, 1H); EI-MS m/z 538 (M^+). HRMS (EI) m/z calcd for M^+ 538.2216; found, 538.2212.

5.1.2.28. *Diethyl 1,1'-(6-aminoquinoxaline-2,3-diyl)dipiperidine-4-carboxylate (12u)*. Diethyl 1,1'-(6-nitroquinoxaline-2,3-diyl)bis(piperidine-4-carboxylate) (**12h**) was treated with 10% Pb/C in MeOH with H_2 . After the reaction was completed, it filtered and concentrated in vacuo to give the product (**12u**). Yield: 91%. mp 185–186 °C. ^1H NMR (300 MHz, $\text{DMSO}-d_6$) δ : 1.27 (t, $J = 13.5$ Hz, 6H), 1.83–1.91 (m, 4H), 2.09 (d, $J = 7.2$ Hz, 4H), 2.44–2.64 (m, 2H), 2.74–2.87 (m, 4H), 4.10 (d, $J = 12$ Hz, 2H), 4.17 (q, $J = 13.5$ Hz, 4H), 4.32 (d, $J = 12$ Hz, 2H), 6.84

(dd, $J_1 = 9$ Hz, $J_2 = 2.7$ Hz, 1H), 6.92 (d, $J = 2.7$ Hz, 1H), 7.51 (d, $J = 9$ Hz, 1H); EI-MS m/z 455 (M^+). HRMS (EI) m/z calcd for M^+ 455.2533; found, 455.2527.

5.1.2.29. *1,1'-(6-Aminoquinoxaline-2,3-diyl)bis(piperidine-4-carboxylic Acid) (12v)*. Diethyl 1,1'-(6-aminoquinoxaline-2,3-diyl)dipiperidine-4-carboxylate (**12u**) was hydrolyzed with 10% NaOH in MeOH. After the reaction was completed, positive ion-exchange resin (Dowex 50w X 4–400) was added to the reaction mixture to neutralize the excess base, filtered, and concentrated in vacuo to give the product (**12v**). Yield: 60%. mp >300 °C. ^1H NMR (400 MHz, $\text{DMSO}-d_6$) δ : 1.63–1.72 (m, 4H), 1.95–1.98 (m, 4H), 2.67–2.80 (m, 4H), 2.98 (d, $J = 12.8$ Hz, 2H), 4.19 (d, $J = 12.8$ Hz, 2H), 6.80 (d, $J = 2.4$ Hz, 1H), 6.87 (dd, $J_1 = 8.8$ Hz, $J_2 = 2.0$ Hz, 1H), 7.38 (d, $J = 8.8$ Hz, 1H); EI-MS m/z 399 (M^+). HRMS (EI) m/z calcd for M^+ 399.1907; found, 399.1915.

5.1.2.30. *7-Nitroquinoxalin-2-ol (9a)*. To a stirred solution of quinoxalin-2-ol **8a** (2.92 g, 20 mmol) in 85 mL of glacial acetic acid was added the mixture of 0.88 mL of concentrated nitric acid and 5 mL of acetic acid in small portions. The resulting solution was stirred at ambient temperature overnight and evaporated, and the residue was then poured into H_2O (50 mL). After half an hour of stirring, the mixture was filtered and washed with water to give compound **9a** (3.22 g, 84%) as a pale yellow solid: mp 273–276 °C. ^1H NMR (500 MHz, $\text{DMSO}-d_6$) δ : 8.00 (s, $J = 8.8$ Hz, 1H), 8.06 (dd, $J_1 = 2.4$ Hz, $J_2 = 8.8$ Hz, 1H), 8.12 (d, $J = 2.4$ Hz, 1H), 8.34 (s, 1H).

5.1.2.31. *6-Nitroquinoxalin-2-ol (9b)*. The powder of KNO_3 (2.0 g, 20 mmol) was added quickly into a mixture of quinoxalin-2-ol **8a** (2.92 g, 20 mmol) in H_2SO_4 (20 mL). The resulting solution was stirred at 0 °C. After half an hour, the mixture was allowed to warm to ambient temperature, stirred for 2 h, and poured into ice (500 mL). The resulting crystals were collected after filtration and washed with water and dried to afford compound **9b** (3.55 g, 93%) as a pale yellow solid: mp 258–260 °C. ^1H NMR (500 MHz, $\text{DMSO}-d_6$) δ : 7.47 (d, $J = 9.0$ Hz, 2H), 8.33 (s, 1H), 8.39 (dd, $J_1 = 2.3$ Hz, $J_2 = 9.0$ Hz, 1H), 8.56 (d, $J = 2.0$ Hz, 1H).

5.1.2.32. *2-Chloro-7-nitroquinoxaline (10a)*. 7-Nitroquinoxalin-2-ol **9a** (0.67 g, 3.6 mmol) was slowly added to POCl_3 (5 mL) and PCl_5 (1.2 g). The reaction mixture was heated under reflux for 4 h. After being cooled to about 20 °C, it was poured into ice water. The solid thus separated as pale pink needles, was filtered, and washed with ice water to give **10a** (0.34 g, 46%) as a gray solid: mp 185–189 °C. ^1H NMR (400 MHz, CDCl_3) δ : 8.31 (d, $J = 9.2$ Hz, 1H), 8.57 (dd, $J_1 = 2.4$ Hz, $J_2 = 9.2$ Hz, 1H), 8.94 (br, 2H).

5.1.2.33. *2-Chloro-6-nitroquinoxaline (10b)*. In the same manner as that described for the preparation of **10a**, **10b** was prepared from 6-nitroquinoxalin-2-ol (**9b**) and POCl_3 . Yield: 39%. mp 197–202 °C. ^1H NMR (400 MHz, CDCl_3) δ : 8.20 (d, $J = 5.2$ Hz, 1H), 8.52 (dd, $J_1 = 1.6$ Hz, $J_2 = 8.8$ Hz, 1H), 8.93 (s, 1H), 9.01 (d, $J = 1.2$ Hz, 1H).

5.1.2.34. *2-Chloroquinoxaline (11a)*. In the same manner as that described for the preparation of **10a**, **11a** was prepared from quinoxalin-2-ol (**8a**) and POCl_3 . Yield: 43%. mp 46–48 °C. ^1H NMR (400 MHz, CDCl_3) δ : 7.78–7.85 (m, 2H), 8.04 (d, $J = 8.4$ Hz, 1H), 8.14 (d, $J = 7.2$ Hz, 1H), 8.80 (s, 1H).

5.1.2.35. *2-Chloroquinoline (11b)*. In the same manner as that described for the preparation of **10a**, **11b** was prepared from quinoline-2-ol (**8b**) and POCl_3 . Yield: 23%. ^1H NMR (400 MHz, CDCl_3) δ : 7.42 (d, $J = 8.8$ Hz, 1H), 7.59 (t, $J = 7.6$ Hz, 1H), 7.75 (t, $J = 7.6$ Hz, 1H), 7.85 (d, $J = 8.0$ Hz, 1H), 8.07 (d, $J = 8.4$ Hz, 1H), 8.14 (d, $J = 8.4$ Hz, 1H).

5.1.2.36. *2-Chlorobenzimidazole (11c)*. In the same manner as that described for the preparation of **10a**, **11c** was prepared from benzimidazole-2-ol (**8c**) and POCl_3 . Yield: 45%. mp 178–180 °C. ^1H NMR (400 MHz, CDCl_3) δ : 7.26 (d, $J = 8.8$ Hz, 1H), 7.70–7.83 (m, 2H).

5.1.2.37. *2-Chloroquinazoline (11d)*. Compound **11d** was prepared following the method reported by Ram et al.³⁴ (see Scheme 1 in Supporting Information for details). Yield: 50%. mp 101–109 °C. ^1H NMR

(400 MHz, CDCl₃) δ : 7.71 (t, J = 8.0 Hz, 1H), 7.97–8.04 (m, 3H), 9.33 (s, 1H).

5.1.2.38. (E)-3-(3-(6-Nitroquinoxalin-3-ylamino)phenyl)acrylic Acid (13a) and (E)-ethyl 3-(3-(6-nitroquinoxalin-3-ylamino)phenyl)acrylate (13c). To a solution of 2-chloro-7-nitroquinoxaline **10a** (209 mg, 1 mmol) in dry DMF (6 mL), (E)-ethyl 3-(3-aminophenyl)acrylate (229 mg, 1.2 mmol) was added. The mixture was refluxed gently for 5 h. DMF was then evaporated under reduced pressure, and the residue was extracted with EtOAc/H₂O three times. The combined organic layer was washed, dried, filtered, and condensed. The residue was purified by flash chromatography on silica gel, eluted with a mixture of EtOAc/petroleum ether (1:6, v/v), to afford (E)-ethyl 3-(3-(6-nitroquinoxalin-3-ylamino)phenyl)acrylate **13c** (182 mg, 57%) as a yellow solid: mp 183–193 °C. ¹H NMR (400 MHz, DMSO-*d*₆) δ : 1.29 (t, J = 7.2 Hz, 3H), 4.23 (q, 2H), 6.60 (d, J = 16.0 Hz, 1H), 7.46–7.47 (m, 2H), 7.71 (d, J = 16.0 Hz, 1H), 8.02–8.03 (m, 1H), 8.06 (d, J = 8.8 Hz, 1H), 8.18 (dd, J_1 = 2.4 Hz, J_2 = 8.8 Hz, 1H), 8.25 (s, 1H), 8.52 (d, J = 2.8 Hz, 1H), 8.70 (s, 1H), 10.37 (s, 1H); EI-MS m/z 364.1 (M⁺). HRMS (EI) m/z calcd C₁₉H₁₆N₄O₄ (M⁺) 364.1172; found, 364.1171.

A mixture of (E)-ethyl 3-(3-(6-nitroquinoxalin-3-ylamino)phenyl)acrylate (45 mg, 0.12 mmol) and LiOH (100 mg, 4.2 mmol) in MeOH (3 mL) was refluxed for 2 h to generate a yellow solution, which was acidified to pH 5.5 after cooling to room temperature. Then the precipitate was collected, washed with H₂O, and dried to afford **13a** (37 mg, 89%) as a yellow solid: mp >300 °C. ¹H NMR (400 MHz, DMSO-*d*₆) δ : 6.52 (d, J = 16.0 Hz, 1H), 7.41–7.48 (m, 2H), 7.64 (d, J = 16.0 Hz, 1H), 8.02–8.06 (m, 2H), 8.17 (dd, J_1 = 2.4 Hz, J_2 = 9.2 Hz, 1H), 8.23 (s, 1H), 8.51 (d, J = 2.0 Hz, 1H), 8.70 (s, 1H), 10.38 (s, 1H); EI-MS m/z 336.1 (M⁺). HRMS (ESI) m/z calcd C₁₇H₁₂N₄O₄ (M⁺) 337.0859; found, 337.0931.

5.1.2.39. (E)-3-(3-(6-Nitroquinoxalin-2-ylamino)phenyl)acrylic Acid (13b). In the same manner as that described for the preparation of **13a**, **13b** was prepared from **10b** and (E)-ethyl 3-(3-aminophenyl)acrylate. Yield: 98%. mp >300 °C. ¹H NMR (400 MHz, DMSO-*d*₆) δ : 6.51 (d, J = 16.0 Hz, 1H), 7.43–7.49 (m, 2H), 7.65 (d, J = 16.0 Hz, 1H), 8.03–8.07 (m, 2H), 8.18 (dd, J_1 = 2.4 Hz, J_2 = 9.2 Hz, 1H), 8.24 (s, 1H), 8.53 (d, J = 2.0 Hz, 1H), 8.72 (s, 1H), 10.42 (s, 1H); EI-MS m/z 336.1 (M⁺). HRMS (EI) m/z calcd C₁₇H₁₂N₄O₄ (M⁺) 336.0859; found, 336.0851.

5.1.2.40. N-(2,3-Dihydrobenzo[b][1,4]dioxin-6-yl)-7-nitroquinoxalin-2-amine (13d). In the same manner as that described for the preparation of **13c**, **13d** was prepared from **10a** and 3,4-ethylenedioxyaniline. Yield: 91%. mp 205–210 °C; ¹H NMR (400 MHz, CDCl₃) δ : 4.25–4.33 (m, 4H), 6.93 (d, J = 8.4 Hz, 1H), 7.06 (dd, J_1 = 2.0 Hz, J_2 = 8.4 Hz, 1H), 7.42 (d, J = 1.2 Hz, 1H), 8.03 (d, J = 9.2 Hz, 1H), 8.22 (dd, J_1 = 2.0 Hz, J_2 = 9.2 Hz, 1H), 8.53 (s, 1H), 8.65 (d, J = 2.0 Hz, 1H); EI-MS m/z 324.1 (M⁺). HRMS (EI) m/z calcd C₁₆H₁₂N₄O₄ (M⁺) 324.0859; found, 324.0854.

5.1.2.41. 5-(6-Nitroquinoxalin-3-ylamino)-2-chlorobenzoic acid (13e). To a stirred solution of the 5-amino-2-chlorobenzoic acid (500 mg) in dry C₂H₅OH (10 mL), cooled to 0 °C, SOCl₂ (0.5 mL) was added dropwise in 5 min. The resulting suspension was then allowed to warm to room temperature with stirring for 1 h and then refluxed for 2 h. The mixture was poured onto sat. NaHCO₃, the phases separated, and the organic phase washed subsequently with sat. NaHCO₃, H₂O, and brine, followed by drying to yield intermediate ethyl 5-amino-2-chlorobenzoate (580 mg, 100%) as a yellow oil. ¹H NMR (400 MHz, CDCl₃) δ : 1.39 (t, J = 7.2 Hz, 3H), 4.40 (q, J_1 = 7.2 Hz, J_2 = 14.4 Hz, 2H), 6.71 (dd, J_1 = 2.8 Hz, J_2 = 8.4 Hz, 1H), 7.10 (d, J = 2.8 Hz, 1H), 7.19 (d, J = 8.8 Hz, 1H).

To a solution of the above intermediate (100 mg, 0.5 mmol) in dry DMF (6 mL), **10a** (125 mg, 0.6 mmol) was added. The mixture was refluxed gently for 2 h. DMF was then evaporated under reduced pressure, and the residue was extracted with EtOAc/H₂O three times. The combined organic layer was washed, dried, filtered, and condensed. The residue was purified by flash chromatography on silica gel, eluted

with a mixture of EtOAc/petroleum ether (1:6, v/v), to afford intermediate ethyl 5-(6-nitroquinoxalin-3-ylamino)-2-chlorobenzoate (89 mg, 48%) as a yellow solid; ¹H NMR (400 MHz, CDCl₃) δ : 1.35 (t, J = 7.2 Hz, 3H), 4.06 (q, J_1 = 7.2 Hz, J_2 = 14.4 Hz, 2H), 7.13 (t, J = 8.0 Hz, 1H), 7.32 (d, J = 8.4 Hz, 1H), 7.41 (d, J = 8.4 Hz, 1H), 7.74 (dd, J_1 = 2.8 Hz, J_2 = 8.8 Hz, 1H), 7.94 (d, J = 2.4 Hz, 1H), 8.13–8.17 (m, 1H), 8.30 (d, J = 1.6 Hz, 1H).

A mixture of ethyl 5-(6-nitroquinoxalin-3-ylamino)-2-chlorobenzoate (89 mg) and LiOH (100 mg, 4.2 mmol) in MeOH (3 mL) was combined at 58 °C for 2 h to generate a yellow solution, which was acidified to pH 5.5 after cooling to room temperature. Then the precipitate was collected, washed with H₂O, and dried to afford **13e** (22 mg, 27%) as an orange solid: mp 161–165 °C. ¹H NMR (400 MHz, DMSO-*d*₆) δ : 7.57 (d, J = 8.8 Hz, 1H), 8.10 (d, J = 8.8 Hz, 1H), 8.22 (dd, J_1 = 2.4 Hz, J_2 = 8.8 Hz, 1H), 8.31 (dd, J_1 = 2.8 Hz, J_2 = 8.8 Hz, 1H), 8.41 (d, J = 6.8 Hz, 1H), 8.48 (d, J = 2.4 Hz, 1H), 8.71 (s, 1H); EI-MS m/z 344.1 (M⁺). HRMS (EI) m/z calcd C₁₅H₉ClN₄O₄ (M⁺) 344.0312; found, 344.0309.

5.1.2.42. N-(3-Ethoxyphenyl)-7-nitroquinoxalin-2-amine (13f). In the same manner as that described for the preparation of **13c**, **13f** was prepared from **10a** and 3-ethoxyaniline. Yield: 95%. mp 166–170 °C. ¹H NMR (400 MHz, DMSO-*d*₆) δ : 1.40 (t, J = 7.2 Hz, 3H), 4.08 (q, 2H), 6.70 (d, J = 7.6 Hz, 1H), 7.08–7.11 (m, 2H), 7.51 (s, 1H), 7.80 (t, J = 8.0 Hz, 1H), 8.20 (s, 1H), 8.52 (s, 1H), 8.63 (t, J = 8.0 Hz, 1H); EI-MS m/z 310.1 (M⁺). HRMS (EI) m/z calcd C₁₆H₁₄N₄O₃ (M⁺) 310.1066; found, 310.1050.

5.1.2.43. 7-Nitro-N-phenylquinoxalin-2-amine (13g). In the same manner as that described for the preparation of **13c**, **13g** was prepared from **10a** and aniline. Yield: 68%. mp 230–233 °C. ¹H NMR (400 MHz, CDCl₃) δ : 7.22 (t, J = 7.2 Hz, 1H), 7.46 (t, J = 7.6 Hz, 1H), 7.76 (d, J = 7.6 Hz, 2H), 8.05 (d, J = 9.2 Hz, 1H), 8.24 (dd, J_1 = 2.8 Hz, J_2 = 9.2 Hz, 1H), 8.56 (s, 1H), 8.67 (d, J = 2.4 Hz, 1H); EI-MS m/z 266.1 (M⁺). HRMS (EI) m/z calcd C₁₄H₁₀N₄O₂ (M⁺) 266.0804; found, 266.0805.

5.1.2.44. 3-(3-(6-Nitroquinoxalin-3-ylamino)phenyl)propanoic Acid (13h). To a solution of 3-(3-aminophenyl)propanoic acid (0.2 g, 1.2 mmol) in 15 mL of EtOH, 0.5 mL of concentrated H₂SO₄ was added. The resulting reaction mixture was refluxed for 2 h. The solvent was removed under reduced pressure, and the residue was partitioned between AcOEt and sat. NaHCO₃. The organic layer was washed with water and brine, dried over anhydrous Na₂SO₄, filtered, and condensed. The crude material could be used in the next step without further purification. ¹H NMR (400 MHz, CDCl₃) δ : 1.27 (t, J = 7.2 Hz, 3H), 2.58 (t, J = 7.6 Hz, 2H), 2.84 (t, J = 8.0 Hz, 2H), 4.18 (q, J_1 = 7.2 Hz, J_2 = 14.4 Hz, 2H), 6.54 (br, 2H), 6.61 (d, J = 7.6 Hz, 1H), 7.07 (t, J = 8.0 Hz, 1H).

To a solution of the above intermediate (100 mg, 0.5 mmol) in dry DMF (3 mL), **10a** (125 mg, 0.6 mmol) was added. The mixture was refluxed gently for 2 h. DMF was then evaporated under reduced pressure, and the residue was extracted with EtOAc/H₂O 3 times. The combined organic layer was washed, dried, filtered, and condensed. The residue was purified by flash chromatography on silica gel, eluted with a mixture of EtOAc/petroleum ether (1:2, v/v), to afford intermediate ethyl 3-(3-(6-nitroquinoxalin-3-ylamino)phenyl)propanoate (130 mg, 75%) as a yellow solid. ¹H NMR (400 MHz, CDCl₃) δ : 1.27 (t, J = 7.2 Hz, 3H), 2.71 (t, J = 7.6 Hz, 2H), 3.03 (t, J = 7.6 Hz, 2H), 4.18 (q, J_1 = 7.2 Hz, J_2 = 14.0 Hz, 2H), 7.06 (d, J = 7.6 Hz, 1H), 7.37 (t, J = 8.0 Hz, 1H), 7.60 (s, 1H), 7.67 (dd, J_1 = 1.6 Hz, J_2 = 8.0 Hz, 1H), 8.04 (d, J = 9.2 Hz, 1H), 8.24 (dd, J_1 = 2.4 Hz, J_2 = 8.8 Hz, 1H), 8.55 (s, 1H), 8.67 (d, J = 2.8 Hz, 1H).

A mixture of ethyl 3-(3-(6-nitroquinoxalin-3-ylamino)phenyl)propanoate (130 mg) and LiOH (100 mg, 4.2 mmol) in MeOH (3 mL) was combined at 58 °C for 2 h to generate a yellow solution, which was acidified to pH 5.5 after cooling to room temperature. Then the precipitate was collected, washed with H₂O, and dried to afford **13h** (59 mg, 49%) as an orange solid: mp 239–245 °C. ¹H NMR (400 MHz,

DMSO- d_6) δ : 2.59 (t, J = 7.6 Hz, 2H), 2.89 (d, J = 7.6 Hz, 2H), 6.97 (d, J = 7.6 Hz, 1H), 7.32 (t, J = 8.0 Hz, 1H), 7.81 (s, 1H), 7.88 (d, J = 8.0 Hz, 1H), 8.05 (d, J = 9.2 Hz, 1H), 8.17 (dd, J_1 = 2.4 Hz, J_2 = 8.8 Hz, 1H), 8.50 (d, J = 2.4 Hz, 1H), 8.70 (s, 1H), 10.26 (s, 1H); EI-MS m/z 338.1 (M^+). HRMS (EI) m/z calcd $C_{17}H_{14}N_4O_4$ (M^+) 338.1015; found, 338.1010.

5.1.2.45. (E)-Ethyl 3-(3-(quinoxalin-3-ylamino)phenyl)acrylate (14c). In the same manner as that described for the preparation of **13c**, **14c** was prepared from **11a** and (E)-ethyl 3-(3-aminophenyl)acrylate. Yield: 90%. mp 110–120 °C. 1H NMR (400 MHz, $CDCl_3$) δ : 1.36 (t, J = 7.2 Hz, 3H), 4.30 (q, 2H), 6.48 (d, J = 16.0 Hz, 1H), 7.25 (d, J = 7.6 Hz, 1H), 7.39 (t, J = 8.0 Hz, 1H), 7.49 (t, J = 8.0 Hz, 1H), 7.65 (t, J = 7.6 Hz, 1H), 7.71 (d, J = 16.0 Hz, 1H), 7.80–7.84 (m, 2H), 7.94 (d, J = 8.0 Hz, 1H), 8.02 (s, 1H), 8.45 (s, 1H); EI-MS m/z 319.2 (M^+). HRMS (EI) m/z calcd $C_{19}H_{17}N_3O_2$ (M^+) 319.1321; found, 319.1316.

5.1.2.46. (E)-3-(3-(Quinoxalin-3-ylamino)phenyl)acrylic Acid (14a). In the same manner as that described for the preparation of **13a**, **14a** was prepared from **14c** and LiOH. Yield: 88%. mp 273–275 °C. 1H NMR (400 MHz, DMSO- d_6) δ : 6.50 (d, J = 16.0 Hz, 1H), 7.38 (d, J = 7.6 Hz, 1H), 7.44 (t, J = 8.0 Hz, 1H), 7.50 (t, J = 8.0 Hz, 1H), 7.62 (d, J = 16.0 Hz, 1H), 7.68 (t, J = 8.0 Hz, 1H), 7.77 (t, J = 8.4 Hz, 1H), 7.88 (d, J = 8.0 Hz, 1H), 8.01 (d, J = 8.0 Hz, 1H), 8.30 (s, 1H), 8.59 (s, 1H), 10.08 (s, 1H), 12.44 (s, 1H); EI-MS m/z 291.1 (M^+). HRMS (EI) m/z calcd $C_{17}H_{13}N_3O_2$ (M^+) 291.1008; found, 291.1010.

5.1.2.47. N-(2,3-Dihydrobenzo[b][1,4]dioxin-6-yl)quinoxalin-2-amine (14b). In the same manner as that described for the preparation of **13c**, **14b** was prepared from **11a** and 3,4-ethylenedioxyaniline. Yield: 33%. mp 133–138 °C. 1H NMR (400 MHz, $CDCl_3$) δ : 4.29–4.30 (m, 4H), 6.89 (d, J = 8.4 Hz, 1H), 7.03 (dd, J_1 = 1.6 Hz, J_2 = 8.4 Hz, 1H), 7.27 (s, 1H), 7.39 (s, 1H), 7.46 (t, J = 8.0 Hz, 1H), 7.63 (t, J = 8.0 Hz, 1H), 7.78 (d, J = 8.4 Hz, 1H), 7.92 (d, J = 8.0 Hz, 1H), 8.42 (s, 1H); EI-MS m/z 279.1 (M^+). HRMS (EI) m/z calcd $C_{16}H_{13}N_3O_2$ (M^+) 279.1008; found, 279.1006.

5.1.2.48. 3-(3-(Quinoxalin-3-ylamino)phenyl)propanoic Acid (14d). In the same manner as that described for the preparation of **13h**, **14d** was prepared from **11a** and 3-(3-aminophenyl)propanoic acid. Yield: 30%. mp 198–201 °C; 1H NMR (400 MHz, DMSO- d_6) δ : 2.59 (t, J = 7.2 Hz, 2H), 2.86 (d, J = 7.2 Hz, 2H), 6.91 (d, J = 6.8 Hz, 1H), 7.28 (t, J = 8.0 Hz, 1H), 7.46 (t, J = 7.6 Hz, 1H), 7.64 (t, J = 7.2 Hz, 1H), 7.74 (d, J = 8.4 Hz, 1H), 7.78 (s, 1H), 7.84–7.89 (m, 2H), 8.55 (s, 1H), 9.89 (s, 1H); EI-MS m/z 293.1 (M^+). HRMS (EI) m/z calcd $C_{17}H_{15}N_3O_2$ (M^+) 293.1164; found, 293.1168.

5.1.2.49. (E)-3-(3-(Quinoxalin-3-yloxy)phenyl)acrylic Acid (14e). To a solution of 3-hydroxycinnamic acid (1 g, 6.1 mmol) in 20 mL of EtOH, 1 mL of concentrated H_2SO_4 was added. The resulting reaction mixture was refluxed for 12 h. The solvent was removed under reduced pressure, and the residue was partitioned between AcOEt and sat. $NaHCO_3$. The organic layer was washed with water and brine, dried over anhydrous Na_2SO_4 , filtered, and condensed to afford a white solid. Yield: 100%. The crude material could be used in the next step without further purification. 1H NMR (400 MHz, $CDCl_3$) δ : 1.36 (t, J = 7.2 Hz, 3H), 4.29 (q, J_1 = 7.2 Hz, J_2 = 14.4 Hz, 2H), 6.42 (d, J = 16.0 Hz, 1H), 6.89 (d, J_1 = 2.0 Hz, J_2 = 8.0 Hz, 1H), 7.03 (s, 1H), 7.12 (d, 1H), 7.28 (t, J = 7.6 Hz, 1H), 7.66 (br, 1H).

To a solution of the above intermediate (150 mg, 0.91 mmol) in dry CCl_4 (5 mL), **11a** (128 mg, 0.78 mmol) and anhydrous K_2CO_3 (250 mg) was added. The mixture was refluxed for 12 h under N_2 . The solution was poured into water and extracted with CH_2Cl_2 . The combined organic phases were washed with 1 N HCl, brine and water, dried, filtered, and concentrated. The residue was purified by flash chromatography on silica gel, eluted with a mixture of EtOAc/petroleum ether (1:6, v/v), to afford intermediate compound (194 mg, 99%) as a pale yellow solid, 1H NMR (400 MHz, $CDCl_3$) δ : 1.35 (t, J = 7.2 Hz, 3H), 4.28 (q, J_1 = 7.2 Hz, J_2 = 14.4 Hz, 2H), 6.47 (d, J = 16.0 Hz, 1H),

7.33 (d, J = 7.2 Hz, 1H), 7.45–7.50 (m, 3H), 7.61–7.74 (m, 3H), 7.78 (br, 1H), 8.10 (d, J = 8.0 Hz, 1H), 8.73 (s, 1H).

A mixture of the above intermediate (55 mg, 0.17 mmol) and LiOH (60 mg, 1.43 mmol) was combined in 4 mL of THF and H_2O mix solvent ($V_{THF}:V_{H_2O} = 3:1$) at 0 °C for 30 h, which was acidified to pH 5.5. Then the precipitate was collected, washed with H_2O , and dried to afford **14e** (32 mg, 64%) as a white solid: mp 165–170 °C. 1H NMR (400 MHz, DMSO- d_6) δ : 6.58 (d, J = 16.0 Hz, 1H), 7.40 (d, J = 8.4 Hz, 1H), 7.54 (t, J = 8.0 Hz, 1H), 7.61 (d, J = 9.6 Hz, 1H), 7.64 (s, 1H), 7.72–7.75 (m, 4H), 8.09 (d, J = 8.0 Hz, 1H), 8.89 (s, 1H), 12.41 (s, 1H); EI-MS m/z 292.1 (M^+). HRMS (EI) m/z calcd $C_{17}H_{12}N_2O_3$ (M^+) 292.0848; found, 292.0850.

5.1.2.50. (E)-2-Methyl-3-(3-(quinoxalin-3-ylamino)phenyl)acrylic Acid (14f). In the same manner as that described for the preparation of **13a**, **14f** was prepared from **11a** and (E)-ethyl 3-(3-aminophenyl)-2-methylacrylate (see Scheme 2 in Supporting Information). Yield: 65%. mp 235–245 °C. 1H NMR (400 MHz, DMSO- d_6) δ : 2.19 (s, 3H), 7.12 (d, J = 8.0 Hz, 1H), 7.42–7.50 (m, 2H), 7.62–7.73 (m, 3H), 7.81 (d, J = 8.0 Hz, 1H), 7.87 (d, J = 8.0 Hz, 1H), 8.37 (s, 1H), 8.57 (s, 1H), 10.04 (s, 1H), 12.51 (s, 1H); EI-MS m/z 305.1 (M^+). HRMS (EI) m/z calcd $C_{18}H_{15}N_3O_2$ (M^+) 305.1164; found, 305.1161.

5.1.2.51. (E)-3-(3-(Quinoxalin-3-ylamino)phenyl)prop-2-en-1-ol (14g). To a solution of (E)-3-(3-aminophenyl)prop-2-en-1-ol (117 mg, 0.71 mmol) (see Scheme 3 in Supporting Information) in dry DMF (5 mL), **11a** (106 mg, 0.71 mmol) and anhydrous K_2CO_3 (300 mg) were added. The mixture was refluxed for 3 h under N_2 . The solution was poured into water and extracted with EtOAc. The combined organic phases were washed with 1 N HCl, brine and water, dried, filtered, and concentrated. The residue was purified by flash chromatography on silica gel, eluted with a mixture of EtOAc/petroleum ether (1:4, v/v), to afford **14g** (30 mg, 16%) as a white solid: mp 90–98 °C. 1H NMR (400 MHz, $CDCl_3$) δ : 5.18 (d, J = 5.6 Hz, 2H), 6.48–6.55 (m, 1H), 6.77 (d, J = 16.0 Hz, 1H), 6.84–6.87 (m, 1H), 6.95–7.05 (m, 2H), 7.19–7.24 (m, 1H), 7.59 (d, J = 8.0 Hz, 1H), 7.70 (t, J = 8.0 Hz, 1H), 7.87 (d, J = 8.8 Hz, 1H), 8.04 (d, J = 8.0 Hz, 1H), 8.53 (s, 1H); EI-MS m/z 277.1 (M^+). HRMS (EI) m/z calcd $C_{17}H_{15}N_3O$ (M^+) 277.1215; found, 277.1216.

5.1.2.52. (E)-3-(3-(Quinolin-2-ylamino)phenyl)acrylic Acid (14h). In the same manner as that described for the preparation of **13a**, **14h** was prepared from **11b** and (E)-ethyl 3-(3-aminophenyl)acrylate. Yield: 50%. mp >300 °C. 1H NMR (400 MHz, DMSO- d_6) δ : 6.60 (d, J = 16.0 Hz, 1H), 7.34 (d, J = 8.8 Hz, 1H), 7.48–7.53 (m, 2H), 7.56 (d, J = 8.0 Hz, 1H), 7.62–7.66 (m, 3H), 7.76 (t, J = 7.6 Hz, 1H), 7.88 (d, J = 7.6 Hz, 1H), 7.94 (d, J = 7.6 Hz, 1H), 8.04 (s, 1H), 8.42 (d, J = 8.8 Hz, 1H), 11.29 (s, 1H); EI-MS m/z 289.1 (M^+). HRMS (EI) m/z calcd $C_{18}H_{14}N_2O_2$ (M^+) 290.1055; found, 290.1048.

5.1.2.53. (E)-3-(3-(1H-Benzo[d]imidazol-2-ylamino)phenyl)acrylic Acid (14i). In the same manner as that described for the preparation of **13a**, **14i** was prepared from **11c** and (E)-ethyl 3-(3-aminophenyl)acrylate. Yield: 48%. mp 271–278 °C. 1H NMR (400 MHz, DMSO- d_6) δ : 6.46 (d, J = 8.0 Hz, 1H), 6.99–7.01 (m, 2H), 7.26 (d, J = 7.6 Hz, 1H), 7.33–7.39 (m, 3H), 7.57 (d, J = 16.0 Hz, 1H), 7.84 (d, J = 8.0 Hz, 1H), 7.97 (s, 1H), 9.54 (s, 1H), 11.05 (s, 1H), 12.38 (s, 1H); EI-MS m/z 279.1 (M^+). HRMS (EI) m/z calcd $C_{16}H_{13}N_3O_2$ (M^+) 279.1008; found, 279.0999.

5.1.2.54. (E)-3-(3-(Quinazolin-2-ylamino)phenyl)acrylic Acid (14j). In the same manner as that described for the preparation of **13a**, **14j** was prepared from **11d** and (E)-ethyl 3-(3-aminophenyl)acrylate. Yield: 58%. mp 225–230 °C. 1H NMR (400 MHz, DMSO- d_6) δ : 6.47 (d, J = 16.0 Hz, 1H), 7.30 (d, J = 7.6 Hz, 1H), 7.36–7.43 (m, 2H), 7.56 (d, J = 16 Hz, 1H), 7.70 (d, J = 8.4 Hz, 1H), 8.34 (t, J = 7.2 Hz, 1H), 7.94 (d, J = 8.0 Hz, 1H), 8.03 (d, J = 7.6 Hz, 1H), 8.29 (s, 1H), 9.34 (s, 1H), 9.96 (s, 1H); EI-MS m/z 291.1 (M^+). HRMS (EI) m/z calcd $C_{17}H_{13}N_3O_2$ (M^+) 291.1008; found, 291.1007.

5.1.2.55. Protein Preparation. *E. coli* strain BL21 cells containing pRSETB-RhoA were grown in 20 mL of LB medium containing ampicillin ($100 \mu\text{g mL}^{-1}$) at 37°C overnight and then inoculated into 1 L of LB supplemented with ampicillin ($100 \mu\text{g mL}^{-1}$). The expression of RhoA was induced by the addition of 0.5 mM of isopropyl β -D-thiogalactoside (IPTG). The cells were harvested by centrifugation at 8,000g, 4°C for 10 min after induction for 6 h at 25°C . The pellet was washed, frozen, and then disrupted by sonication against the binding buffer (20 mM Tris-HCl, 0.5 M NaCl, and 10 mM imidazole, pH 8.0). The lysate was centrifuged at 18,000g for 30 min at 4°C to pellet the cellular debris. The supernatant was then added to a HiTrap Ni²⁺ chelating column (1 mL) pre-equilibrated with the binding buffer, followed by washing with 20 mL of washing buffer (20 mM Tris-HCl, 0.5 M NaCl, and 60 mM imidazole, pH 8.0). The protein of interest was eluted with 10 mL of elution buffer (20 mM Tris-HCl, 0.5 M NaCl, and 300 mM imidazole, pH 8.0). The freshly prepared protein was dialyzed against the appropriate buffer as required. The purified RhoA was concentrated by Amicon Ultra-4 centrifugal filter devices (Millipore) with the molecular cutoff at 10 kDa. The purity and molecular weights of RhoA were verified by SDS-PAGE.

5.1.2.56. Cell Culture. Human brain vascular smooth muscle cells were maintained at 37°C in a humidified atmosphere composed of 95% air/5% CO₂, grown in DMEM medium supplemented with 10% FBS, 100 U/mL penicillin, and 100 $\mu\text{g/mL}$ streptomycin. The culture medium was changed every other day until subculture. All of the experiments were performed using the same primary cell cultures after 3 to 6 passages being seeded into T-25 culture flasks.

5.1.2.57. Tissue Preparation. All protocols involving the use of animals were approved by the University of Sochow Animal Care and Use Committee. Adult male Sprague-Dawley rat weighing 270–320 g were killed by cervical dislocation in compliance. The thoracic aorta arteries were collected in an ice-cold modified Krebs-Henseleit bicarbonate solution (Modified K-H, in mM, 120 NaCl, 4.5 KCl, 1 MgSO₄, 27 NaHCO₃, 1.2 KH₂PO₄, 2.5 CaCl₂, and 10 glucose, and bubbled with 95%O₂–5%CO₂), cleaned of adventitial and adherent connective tissues, and cut in 4- to 5-mm-length rings. We carefully removed the endothelium by gently rubbing the intimal surface with the tip of small forceps.

■ ASSOCIATED CONTENT

Supporting Information. General information for chemical agents and analytical measurements, kinetic analysis of RhoA/inhibitor binding by surface plasmon resonance, the ranks of the three hit compounds identified from the top 3000 docking candidates, the detailed synthetic procedures and related spectroscopic data for compound **11d** and starting material of compounds **14f** and **14g**, and HPLC reports for the purity check of the compounds **1**, **12a–v**, **13a–h**, and **14a–j**. This material is available free of charge via the Internet at <http://pubs.acs.org>.

■ AUTHOR INFORMATION

Corresponding Author

*E-mail: (L.M.) miaolysuzhou@163.com; (H.L.) hlli@ecust.edu.cn. (J.L.) Phone: +86-21-64252584. Fax: +86-21-64252584. E-mail: jianli@ecust.edu.cn.

Author Contributions

[†]These authors contributed equally to this work.

■ ACKNOWLEDGMENT

We gratefully acknowledge the financial supports from the National Natural Science Foundation of China (Grants 90813005

and 20902022), National S&T Major Project, China (Grant 2009ZX09S01-001 and 2011ZX09102-005-02), the Natural Science Foundation of Jiangsu Province (Grant BK2008172), the 111 Project (Grant B07023), and the Fundamental Research Funds for the Central Universities.

■ ABBREVIATIONS USED

ROCK, Rho-associated, coiled-coil containing protein kinase; MLCK, myosin light chain kinase; MLCP, myosin light chain phosphatase; SPR, surface plasmon resonance; PE, phenylephrine; PDB, protein data bank; SAR, structure-activity relationship; DMSO, dimethyl sulfoxide; EDC, *N*-ethyl-*N'*-dimethylamino-propyl carbodiimide; NHS, *N*-hydroxysuccinimide; DMEM, Dulbecco's modified Eagle's medium; FBS, fetal bovine serum; LPA, oleoyl- α -lysophosphatidic acid; RU, response units; IC₅₀, half maximal inhibitory concentration; DCM, dichloromethane; DMF, *N,N*-dimethylformamide; IPTG, isopropyl β -D-thiogalactoside

■ REFERENCES

- (1) Pérez, L.; Danishefsky, S. J. Chemistry and biology in search of antimetastatic agents. *ACS Chem. Biol.* **2009**, *3*, 159–162.
- (2) Sehr, P.; Joseph, G.; Genth, H.; Just, I.; Pick, E.; Aktories, K. Glucosylation and ADP ribosylation of Rho proteins: Effects on nucleotide binding, GTPase activity, and effector coupling. *Biochemistry* **1998**, *37*, 5296–5304.
- (3) Etienne-Manneville, S.; Hall, A. Rho GTPases in cell biology. *Nature* **2002**, *420*, 629.
- (4) Wheeler, A. P.; Ridley, A. J. Why three Rho proteins? RhoA, RhoB, RhoC, and cell motility. *Exp. Cell Res.* **2004**, *301*, 43–49.
- (5) Sander, E. E.; Collard, J. G. Rho-like GTPases: Their role in epithelial cell-cell adhesion and invasion. *Eur. J. Cancer* **1999**, *35*, 1302–1308.
- (6) Ridley, A. J. Rho family proteins: Coordinating cell responses. *Trends Cell Biol.* **2001**, *11*, 471–477.
- (7) Budzyn, K.; Marley, P. D.; Sobey, C. G. Targeting Rho and Rho-kinase in the treatment of cardiovascular disease. *Trends Pharmacol. Sci.* **2006**, *27*, 97–104.
- (8) Uehata, M.; Ishizaki, T.; Satoh, H.; Ono, T.; Kawahara, T.; Morishita, T.; Tamakawa, H.; Yamagami, K.; Inui, J.; Maekawa, M.; Narumiya, S. Calcium sensitization of smooth muscle mediated by a Rho-associated protein kinase in hypertension. *Nature* **1997**, *389*, 990–994.
- (9) Somlyo, A. P.; Somlyo, A. V. Ca²⁺ sensitivity of smooth muscle and nonmuscle myosin II: Modulated by G proteins, kinases, and myosin phosphatase. *Physiol. Rev.* **2003**, *83*, 1325–1358.
- (10) Budzyn, K.; Marley, P. D.; Sobey, C. G. Targeting Rho and Rho-kinase in the treatment of cardiovascular disease. *Trends Pharmacol. Sci.* **2006**, *27*, 97–104.
- (11) Nossaman, B. D.; Kadowitz, P. J. The role of the RhoA/rho-kinase pathway in pulmonary hypertension. *Curr. Drug Discovery Technol.* **2009**, *6*, 59–71.
- (12) Rolfe, B. E.; Worth, N. F.; World, C. J.; Campbell, J. H.; Campbell, G. R. Rho and vascular disease. *Atherosclerosis* **2005**, *183*, 1–16.
- (13) Greenberg, D. L.; Mize, G. J.; Takayama, T. K. Protease-activated receptor mediated RhoA signaling and cytoskeletal reorganization in LNCaP cells. *Biochemistry* **2003**, *42*, 702–709.
- (14) Lu, Q.; Longo, F. M.; Zhou, H.; Massa, S. M.; Chen, Y. H. Signaling through Rho GTPase pathway as viable drug target. *Curr. Med. Chem.* **2009**, *16*, 1355–1365.
- (15) Denoyelle, C.; Albanese, P.; Uzanb, G.; Li, H.; Vannier, J. P.; Soria, J.; Soria, C. Molecular mechanism of the anti-cancer activity of cerivastatin, an inhibitor of HMG-CoA reductase, on aggressive human breast cancer cells. *Cell. Signalling* **2003**, *15*, 327–338.

- (16) Karlsson, R.; Pedersen, E. D.; Wang, Z.; Brakebusch, C. Rho GTPase function in tumorigenesis. *Biochim. Biophys. Acta* **2009**, *1796*, 91–98.
- (17) Kitaoka, Y.; Kitaoka, Y.; Kumai, T.; Lamb, T. T.; Kuribayashi, K.; Isenoumi, K.; Munemasa, Y.; Motoki, M.; Kobayashi, S.; Ueno, S. Involvement of RhoA and possible neuroprotective effect of fasudil, a Rho kinase inhibitor, in NMDA-induced neurotoxicity in the rat retina. *Brain Res.* **2004**, *1018*, 111–118.
- (18) Chiba, Y.; Todoroki, M.; Misawa, M. Interleukin-4 upregulates RhoA protein via an activation of STAT6 in cultured human bronchial smooth muscle cells. *Pharmacol. Res.* **2010**, *61*, 188–192.
- (19) Chang, H. R.; Huang, H. P.; Kao, Y. L.; Chen, S. L.; Wu, S. W.; Hung, T. W.; Lian, J. D.; Wang, C. J. The suppressive effect of Rho kinase inhibitor, Y-27632, on oncogenic Ras/RhoA induced invasion/migration of human bladder cancer TSGH cells. *Chem.-Biol. Interact.* **2010**, *183*, 172–180.
- (20) Takami, A.; Iwakubo, M.; Okada, Y.; Kawata, T.; Odai, H.; Takahashi, N.; Shindo, K.; Kimura, K.; Tagami, Y.; Miyake, M.; Fukushima, K.; Inagaki, M.; Amano, M.; Kaibuchi, K.; Iijima, H. Design and synthesis of Rho kinase inhibitors (I). *Bioorg. Med. Chem.* **2004**, *12*, 2115–2137.
- (21) Goodman, K. B.; Cui, H.; Dowdell, S. E.; Gaitanopoulos, D. E.; Ivy, R. L.; Sehon, C. A.; Stavenger, R. A.; Wang, G. Z.; Viet, A. Q.; Xu, W.; Ye, G.; Semus, S. F.; Evans, C.; Fries, H. E.; Jolivet, L. J.; Kirkpatrick, R. B.; Dul, E.; Khandekar, S. S.; Yi, T.; Jung, D. K.; Wright, L. L.; Smith, G. K.; Behm, D. J.; Bentley, R.; Doe, C. P.; Hu, E.; Lee, D. Development of dihydropyridone indazole amides as selective Rho-kinase inhibitors. *J. Med. Chem.* **2007**, *50*, 6–9.
- (22) Stavenger, R. A.; Cui, H.; Dowdell, S. E.; Franz, R. G.; Gaitanopoulos, D. E.; Goodman, K. B.; Hilfiker, M. A.; Ivy, R. L.; Leber, J. D.; Marino, J. P.; Oh, H.-J.; Viet, A. Q.; Xu, W.; Ye, G.; Zhang, D.; Zhao, Y.; Jolivet, L. J.; Head, M. S.; Semus, S. F.; Elkins, P. A.; Kirkpatrick, R. B.; Dul, E.; Khandekar, S. S.; Yi, T.; Jung, D. K.; Wright, L. L.; Smith, G. K.; Behm, D. J.; Doe, C. P.; Bentley, R.; Chen, Z. X.; Hu, E.; Lee, D. Discovery of aminofurazan-azabenzimidazoles as inhibitors of Rho-kinase with high kinase selectivity and antihypertensive activity. *J. Med. Chem.* **2007**, *50*, 2–5.
- (23) Sehon, C. A.; Wang, G. Z.; Viet, A. Q.; Goodman, K. B.; Dowdell, S. E.; Elkins, P. A.; Semus, S. F.; Evans, C.; Jolivet, L. J.; Kirkpatrick, R. B.; Dul, E.; Khandekar, S. S.; Yi, T.; Wright, L. L.; Smith, G. K.; Behm, D. J.; Bentley, R.; Doe, C. P.; Hu, E.; Lee, D. Potent, selective and orally bioavailable dihydropyrimidine inhibitors of Rho kinase (ROCK1) as potential therapeutic agents for cardiovascular diseases. *J. Med. Chem.* **2008**, *51*, 6631–6634.
- (24) Feng, Y.; Yin, Y.; Weiser, A.; Griffin, E.; Cameron, M. D.; Lin, L.; Ruiz, C.; Schurer, S. C.; Inoue, T.; Rao, P. V.; Schroter, T.; LoGrasso, P. Discovery of substituted 4-(pyrazol-4-yl)-phenylbenzodioxane-2-carboxamides as potent and highly selective Rho kinase (ROCK-II) inhibitors. *J. Med. Chem.* **2008**, *51*, 6642–6645.
- (25) Wilde, C.; Aktories, K. The Rho-ADP-ribosylating C3 exoenzyme from *Clostridium botulinum* and related C3-like transferases. *Toxicon* **2001**, *39*, 1647–1660.
- (26) Vogelsgesanga, M.; Stieglitz, B.; Herrmann, C.; Pautsch, A.; Aktories, K. Crystal structure of the *Clostridium limosum* C3 exoenzyme. *FEBS Lett.* **2008**, *582*, 1032–1036.
- (27) Han, S.; Arvai, A. S.; Clancy, S. B.; Tainer, J. A. Crystal structure and novel recognition motif of Rho ADP-ribosylating C3 exoenzyme from *Clostridium botulinum*: Structural insights for recognition specificity and catalysis. *J. Mol. Biol.* **2001**, *305*, 95–107.
- (28) Tan, E. Y. M.; Law, J. W. S.; Wang, C. H.; Lee, A. Y. W. Development of a cell transducible RhoA inhibitor TAT–C3 transferase and its encapsulation in biocompatible microspheres to promote survival and enhance regeneration of severed neurons. *Pharm. Res.* **2007**, *24*, 2297–2308.
- (29) Lord-Fontaine, S.; Yang, F.; Diep, Q.; Dergham, P.; Munzer, S.; Tremblay, P.; McKerracher, L. Local inhibition of Rho signaling by cell-permeable recombinant protein BA-210 prevents secondary damage and promotes functional recovery following acute spinal cord injury. *J. Neurotraum.* **2008**, *25*, 1309–1322.
- (30) Town, L. J.; Simpson, F.; McGlenn, E. C.; Butterfield, N.; Richman, J. M.; Wicking, C. A novel RhoA inhibitor implicated in lip and palate formation. *Dev. Biol.* **2007**, *306*, 447–447.
- (31) Ewing, T. J. A.; Makino, S.; Skillman, A. G.; Kuntz, I. D. DOCK 4.0: search strategies for automated molecular docking of flexible molecule databases. *J. Comput.-Aided Mol. Des.* **2001**, *15*, 411–428.
- (32) Meng, E. C.; Shoichet, B. K.; Kuntz, I. D. Automated docking with grid-based energy evaluation. *J. Comput. Chem.* **1992**, *13*, 505–524.
- (33) Hyvelin, J. M.; O'Connor, C.; McLoughlin, P. Effect of changes in pH on wall tension in isolated rat pulmonary artery: role of the RhoA/Rho-kinase pathway. *Am. J. Physiol. Lung Cell Mol. Physiol.* **2004**, *287*, L673–684.
- (34) Ram, V. J.; Farhanullah; Tripathi, B. K.; Srivastava, A. K. Synthesis and antihyperglycemic activity of suitably functionalized 3H-quinazolin-4-one. *Bioorg. Med. Chem.* **2003**, *11*, 2439–2444.